SOLAR ENERGY

THE JOURNAL OF SOLAR ENERGY SCIENCE AND ENGINEERING

VOLUME IV | OCTOBER, 1960 | NUMBER 4

VOL. 4 1960

PUBLISHED QUARTERLY BY
THE ASSOCIATION FOR APPLIED SOLAR ENERGY
ARIZONA STATE UNIVERSITY, TEMPE, ARIZONA

EXECUTIVE COMMITTEE

H. WALMSLEY, *President*
Brig. Gen., USA Retired
JAN OOSTERMEYER, *Vice President*
Retired President, Shell Chemical Corporation
WALTER T. LUCKING, *Vice President*
President, Arizona Public Service Company
HENRY SARGENT, *Vice President*
President, American & Foreign Power Co., New York
WALTER BIMSON
Chairman of the Board, Valley National Bank
WELDON B. GIBSON
Vice President, Stanford Research Institute
SHERMAN HAZELTINE
Chairman of the Board, First Nat'l Bank of Arizona
G. ROBERT HERBERGER
Chairman of the Board, G. R. Herberger's Inc.
JOHN M. JACOBS
Owner, John Jacobs Farms
JOHN MILLS
Chairman of the Board, Associated Federal Hotels
FRANK SNELL
Partner, Snell & Wilmer

EDITORIAL BOARD

A. B. Stafford, *Editor*
Sidney W. Wilcox, *Assoc. Editor*

ADVISORY AND CONTRIBUTING EDITORS

JOHN P. DECKER
U.S. Forest Service
FRANK E. EDLIN
E. I. DuPont de Nemours & Co.
MERRITT KASTENS
Union Carbide International
RUSSELL L. RIESE
Arizona State University

SUBSCRIPTIONS

The Journal is sent to AFASE members as one of their membership benefits. Non-members may purchase single copies of this issue at $3 per copy, or may obtain a subscription at $10 per year. Please send all communications and inquiries regarding back numbers, dues, etc., to AFASE at the above address. All correspondence regarding manuscripts should be addressed to A. B. Stafford, Arizona State University.

TABLE OF CONTENTS

Optical Characteristics of Silicon Solar Cells and of Coatings for Temperature Control 1
C. A. Escoffery and Werner Luft

Solar Space Heating and Air Conditioning in the Thomason Home 11
Harry E. Thomason

Survey of Electron Transfer Spectra of Inorganic Ions 20
Rudolph J. Marcus

Selectively Emissive Materials for Solar Heat-Absorbers 24
R. B. Gillette

Randomly Rotating, Spherically Arrayed Silicon Solar Energy Converters 33
Werner Luft

Solar Abstracts 40

Index of Articles Published in Solar Energy, Volumes I–IV, 1956 thru 1960 45

Cover Photo: Picture by Josef Muench

SOLAR ENERGY

THE JOURNAL OF SOLAR ENERGY SCIENCE AND ENGINEERING

VOLUME IV | OCTOBER, 1960 | NUMBER 4

VOL. 4 1960

PUBLISHED QUARTERLY BY
THE ASSOCIATION FOR APPLIED SOLAR ENERGY
ARIZONA STATE UNIVERSITY, TEMPE, ARIZONA

EXECUTIVE COMMITTEE

H. WALMSLEY, *President*
Brig. Gen., USA Retired
JAN OOSTERMEYER, *Vice President*
Retired President, Shell Chemical Corporation
WALTER T. LUCKING, *Vice President*
President, Arizona Public Service Company
HENRY SARGENT, *Vice President*
President, American & Foreign Power Co., New York
WALTER BIMSON
Chairman of the Board, Valley National Bank
WELDON B. GIBSON
Vice President, Stanford Research Institute
SHERMAN HAZELTINE
Chairman of the Board, First Nat'l Bank of Arizona
G. ROBERT HERBERGER
Chairman of the Board, G. R. Herberger's Inc.
JOHN M. JACOBS
Owner, John Jacobs Farms
JOHN MILLS
Chairman of the Board, Associated Federal Hotels
FRANK SNELL
Partner, Snell & Wilmer

EDITORIAL BOARD

A. B. Stafford, *Editor*
Sidney W. Wilcox, *Assoc. Editor*

ADVISORY AND CONTRIBUTING EDITORS

JOHN P. DECKER
U.S. Forest Service
FRANK E. EDLIN
E. I. DuPont de Nemours & Co.
MERRITT KASTENS
Union Carbide International
RUSSELL L. RIESE
Arizona State University

SUBSCRIPTIONS

The Journal is sent to AFASE members as one of their membership benefits. Non-members may purchase single copies of this issue at $3 per copy, or may obtain a subscription at $10 per year. Please send all communications and inquiries regarding back numbers, dues, etc., to AFASE at the above address. All correspondence regarding manuscripts should be addressed to A. B. Stafford, Arizona State University.

TABLE OF CONTENTS

Optical Characteristics of Silicon Solar Cells and of Coatings for Temperature Control 1
C. A. Escoffery and Werner Luft

Solar Space Heating and Air Conditioning in the Thomason Home 11
Harry E. Thomason

Survey of Electron Transfer Spectra of Inorganic Ions 20
Rudolph J. Marcus

Selectively Emissive Materials for Solar Heat-Absorbers 24
R. B. Gillette

Randomly Rotating, Spherically Arrayed Silicon Solar Energy Converters 33
Werner Luft

Solar Abstracts 40

Index of Articles Published in Solar Energy, Volumes I–IV, 1956 thru 1960 45

Cover Photo: Picture by Josef Muench

Optical Characteristics of Silicon Solar Cells and of Coatings for Temperature Control

C. A. Escoffery and Werner Luft

International Rectifier Corporation, El Segundo, California

Silicon photovoltaic cells, which are widely used in space vehicles for the direct conversion of solar radiation into electric power, exhibit an undesirable decrease in power output with increase in cell temperature. This article discusses the control of cell temperature in terms of the absorptance and the emittance of solar radiation by the cell surface. Using measured values of spectral reflectance to 25 microns, these parameters are determined for uncovered cells and for cells provided with glass filters and with silicon oxide films.

INTRODUCTION

Ever since its discovery,[1] the silicon *p-n* junction photovoltaic cell, also known as the solar cell, has been the subject of considerable interest. At present, as the most efficient photovoltaic converter of solar energy, it is extensively used in space vehicles, and in various terrestrial applications.[2]

The theory of the photovoltaic effect has been reviewed by various authors.[3-7] A solar cell consists essentially of a *p-n* junction located close to the top exposed surface. Photons with energies greater than the band gap of silicon are capable of being absorbed in the silicon crystal to liberate electron-hole pairs. These excess current carriers diffuse, and those that are separated by the built-in junction potential give rise to a voltage across the cell terminals. If the latter are connected by an external circuit, an electric current will flow and can do useful work.

Fig. 1 shows the spectral response of the silicon solar cell, and Fig. 2 illustrates the influence of temperature on the voltage-current characteristics. Since the power output of the cell decreases with increase in temperature, it is important that the cell temperature rise be minimized through careful design of the solar energy converter system.

One of the widest applications for silicon solar cells is to supply auxiliary power in space vehicles. The cells are usually attached to large sections of the vehicle and absorb most of the solar energy received, but only 10 per cent or less of this energy is converted into electricity, the rest heating the cells and the space vehicle. This heat raises the cell temperature and serves to reduce the energy conversion efficiency even further.

The only way to dissipate the heat in space is by radiation. Consequently, the cell temperature is determined mainly by the optical characteristics of the solar cell surface.

OPTICAL CHARACTERISTICS OF UNCOVERED SILICON SOLAR CELLS

The spectral absorptance, α_λ, of the solar cell is defined as the ratio of the energy absorbed at each wave length to that absorbed by a blackbody at the same temperature. Likewise, the spectral emittance, ϵ_λ, of the solar cell is defined as the ratio of the energy emitted at each wave length to that emitted by a blackbody at the same temperature.

By Kirchoff's law, α_λ and ϵ_λ are equal, and since the solar cell is opaque, they can be computed from measurements of spectral reflectance* by subtracting from unity. Figs. 3 and 4 illustrate typical room-temperature spectral reflectance values for silicon solar cells manufactured by International Rectifier Corporation.

Fig. 3 shows that in the spectral region where the cells are effective converters, the reflectance is quite low, for instance less than 4% at 0.75 microns. (Some cells have shown a reflectance at 0.75 microns as low as 2%). This low reflectance is not characteristic of silicon, which is usually considered to have a value of 30% or more in this spectral region.[10-13] On the other hand, as shown in Fig. 4, the solar cells unfortunately have a high reflectance at long wave lengths, where

* Throughout this discussion, the term reflectance indicates the value at near-normal incidence. Spectral reflectance values are generally constant up to at least 15°, the departure at higher angles depending on the wave length, the material, and the surface condition. Theoretically, therefore, α_λ and ϵ_λ are also angular dependent,[8] but to a first approximation this dependence has been neglected in equations [1-5].

Most of the reflectance measurements shown in the several figures of this report were made by Dunkle[9] and associates at the University of California, Berkeley, California; transmission measurements were made by Optical Coating Laboratory, Santa Rosa, California.

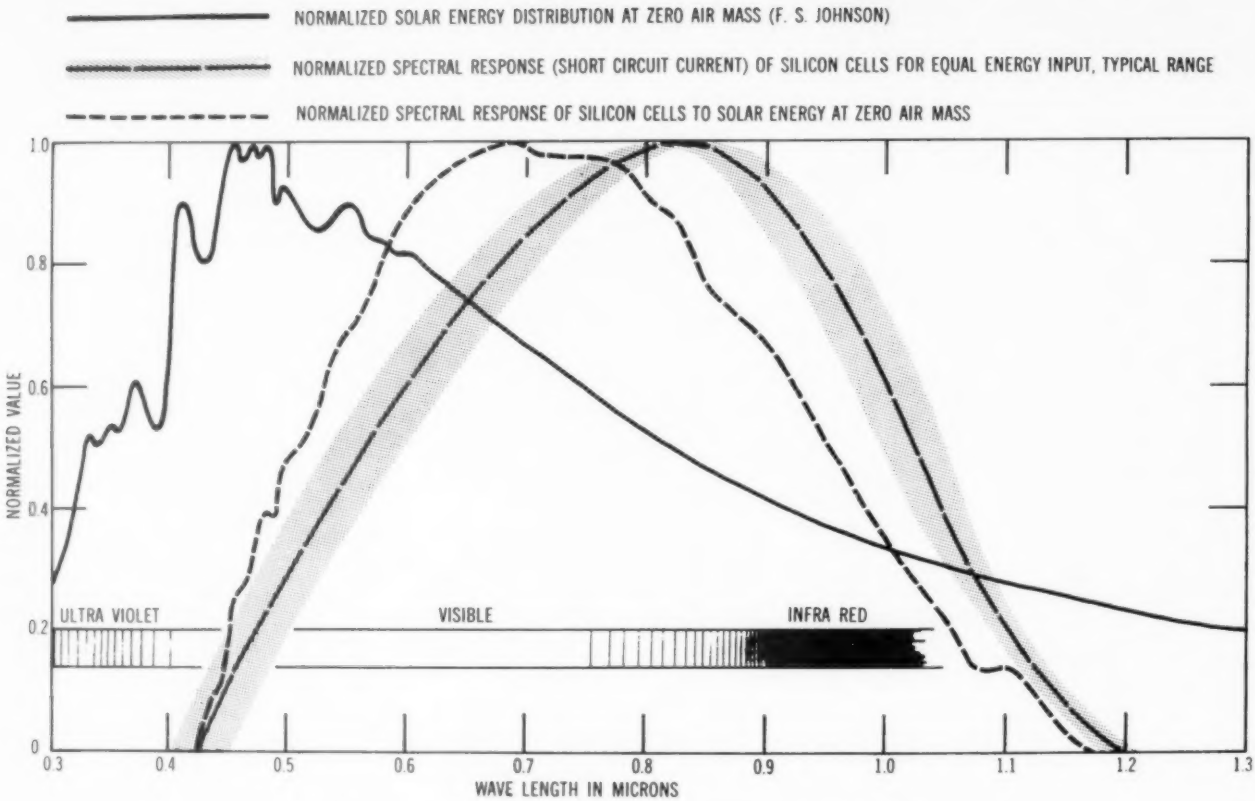

FIG. 1—Solar radiation and spectral response of solar cells.

maximum emitted radiation takes place. It is probable that the boron used in doping creates a silicon alloy with "semi-metal" characteristics.[14]

Absorptance

The average total absorptance for solar radiation, $\bar{\alpha}_S$, of a surface exposed to such radiation is defined as the ratio of the total solar energy absorbed to that absorbed by a blackbody at the same temperature.* With respect to solar radiation in space, it is approximately given by the following equation:

$$\bar{\alpha}_S = \frac{\int_0^\infty \alpha_\lambda I_\lambda \, d\lambda}{\int_0^\infty I_\lambda \, d\lambda} \qquad [1]$$

where I_λ is the solar radiation intensity at each wave length, and α_λ is the spectral absorptance.

For solar radiation just outside the atmosphere (airmass = 0), Equation [1] can be approximated by:

$$\bar{\alpha}_S = \frac{\int_0^{2.5} \alpha_\lambda I_\lambda \, d\lambda}{\int_0^{2.5} I_\lambda \, d\lambda} \qquad [2]$$

since over 96 per cent of the solar energy resides in the range 0.2 to 2.5 microns.[15]

Equation [2] has been evaluated through point by point multiplication of Johnson's curve[15] for solar radiation (Fig. 1) and values of spectral absorptance (Figs. 3 and 4), the integral then being determined with a planimeter. For silicon solar cells made by International Rectifier Corporation, the average solar absorptance, is about 0.93.

Emittance

The average total emittance, $\bar{\epsilon}_T$, of a surface at temperature T is defined as the ratio of the integrated value of the energy emitted at each wave length by the surface to that emitted by a blackbody at the same temperature. To a first approximation, it is given by

$$\bar{\epsilon}_T = \frac{\int_0^\infty \epsilon_\lambda W_{\lambda T} \, d\lambda}{\int_0^\infty W_{\lambda T} \, d\lambda} \qquad [3]$$

where $W_{\lambda T}$ is the radiant flux density emitted per unit wave length increment at wave length λ by a blackbody at temperature T, and ϵ_λ is the spectral emittance.

Because spectral data of ϵ_λ above 25 microns for solar cells are not available, Equation [3] is approxi-

* Actually, $\bar{\alpha}_S$, is also a slight function of temperature, but since for our purposes the temperature coefficient is believed to be negligible, the subscript T is omitted in the interest of simplicity.

VOL. 4 1960

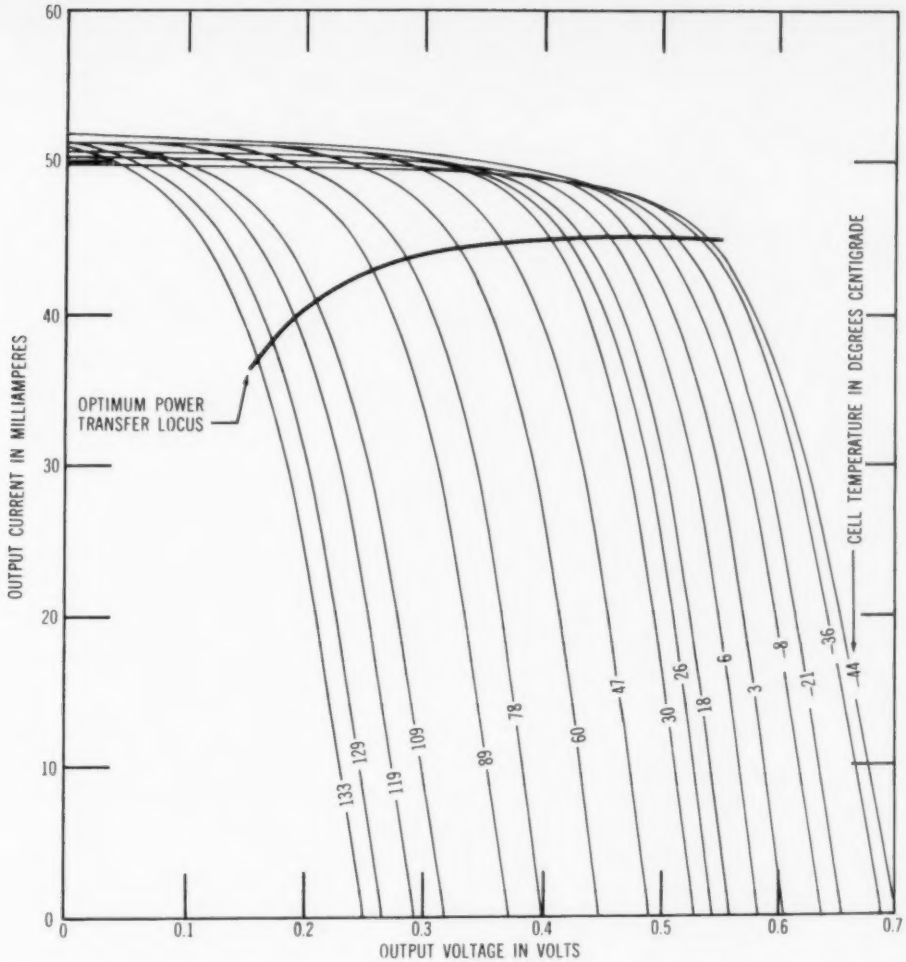

FIG. 2—Temperature dependence of the voltage-current characteristics of a silicon solar cell (1 x 2 cm size) with 10% conversion efficiency at 100 mw cm^{-2} solar radiation.

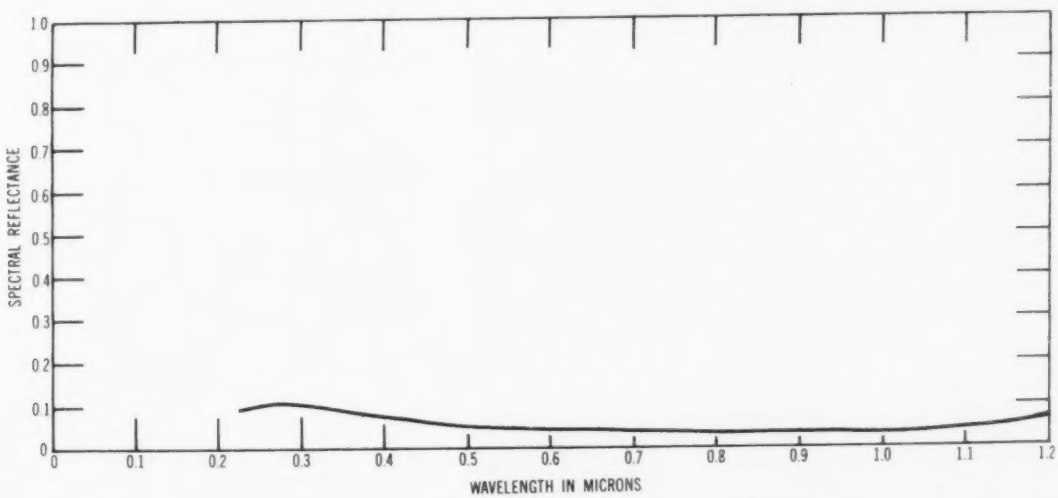

FIG. 3—Spectral reflectance below 1.2 microns for borondoped silicon solar cell surface.

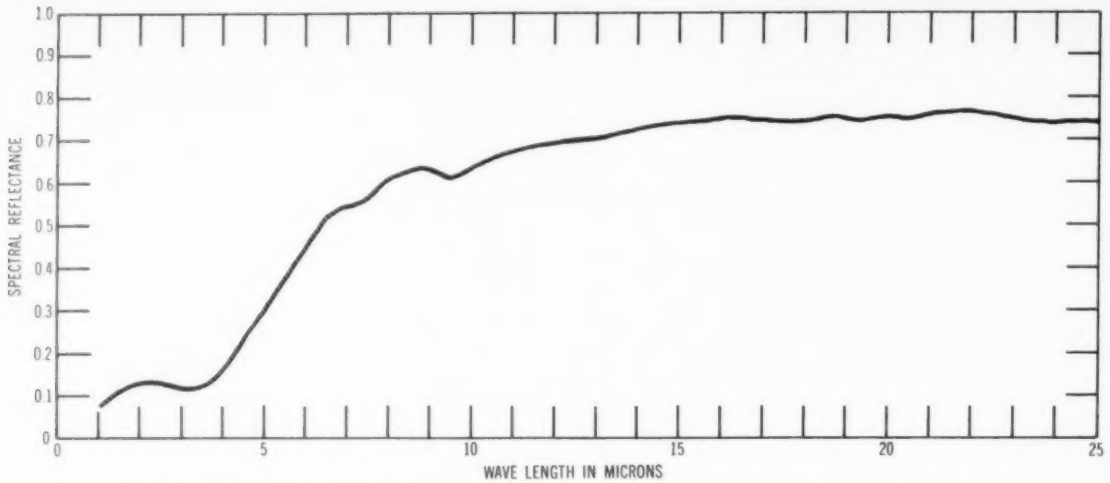

FIG. 4—Spectral reflectance above 1 micron for boron-doped silicon solar cell surface.

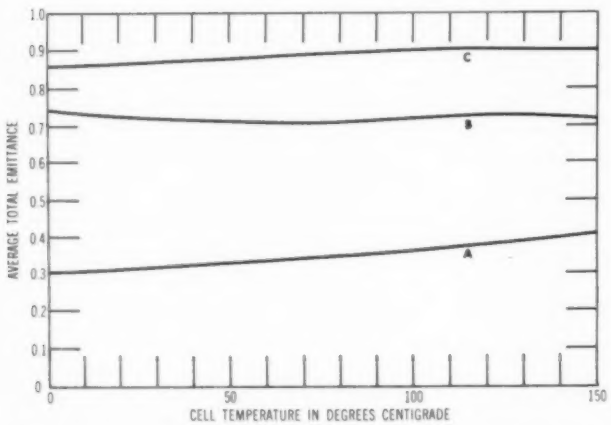

FIG. 5—Average total emittance vs. temperature for various solar cell surfaces. (See Table II for description.)

mated by the following:

$$\bar{\epsilon}_T = \frac{\int_0^{25} \epsilon_\lambda W_{\lambda T}\, d\lambda}{\int_0^{25} W_{\lambda T}\, d\lambda} \cdot q + \epsilon'(1 - q) \qquad [4]$$

where q is the ratio of the radiant flux emitted between 0 and 25 microns to the total radiant flux emitted, and ϵ' is a constant determined by extrapolation of ϵ_λ above 25 microns.

The value of q in Equation [4] is 80, 86, 90, and 92.5 % for surface temperatures of 0, 50, 100, and 150 C, respectively. Values of $\bar{\epsilon}_T$ were not calculated below 0 C, since due to the decreasing value of q, the second term in Equation [4] increases, with a corresponding increase in the uncertainty of the calculation.

Using values of spectral emittance obtained from Fig. 4 and Planckian blackbody distribution curves for different temperatures, Equation [4] was evaluated. For silicon solar cells manufactured by International Rectifier Corporation, the average total emittance, $\bar{\epsilon}_T$ is about 0.30–0.40, as illustrated by Fig. 5, curve A.

CONTROL OF SOLAR CELL TEMPERATURE IN SPACE ENVIRONMENT

The optical characteristics of the space vehicle, and especially of the solar cells, play a determining role in the design of the solar energy converter system. It can be shown that the temperature of any surface element in orbit about the earth is approximately given by:

$$T = \left\{ \frac{1 - f}{\sigma} \left[\left(\frac{A_\alpha}{A_\epsilon} \right)_S \left(\frac{\bar{\alpha}_S}{\bar{\epsilon}_T} \right) C_1 + \left(\frac{A_\alpha}{A_\epsilon} \right)_E \left(\frac{\bar{\alpha}_S}{\bar{\epsilon}_T} \right) C_2 + \left(\frac{A_\alpha}{A_\epsilon} \right)_E \left(\frac{\bar{\alpha}_E}{\bar{\epsilon}_T} \right) C_3 \right] \right\}^{1/4} \qquad [5]$$

where T = equilibrium temperature (°K)
f = fraction of incident energy dissipated elsewhere
σ = Stefan-Boltzmann's constant (5.67×10^{-8} $wm^{-2}K^{-4}$)
A_α = projected absorbing area (m^2)
A_ϵ = emitting area (m^2)
$\bar{\alpha}_S$ = average absorptance for solar radiation
$\bar{\alpha}_E$ = average absorptance for earth radiation
$\bar{\epsilon}_T$ = average total emittance of element at temperature T
C_1 = direct solar irradiation (wm^{-2})
C_2 = earth reflected solar radiation (wm^{-2})
C_3 = earth long wave radiation (wm^{-2})

and subscripts S and E refer to sun and earth, respectively.

Equation [5] assumes that heat transfer is accomplished only by radiation (no conduction of heat to or from the element by adjacent parts). Furthermore, it is assumed that no net radiation exchange occurs be-

VOL. 4 1960

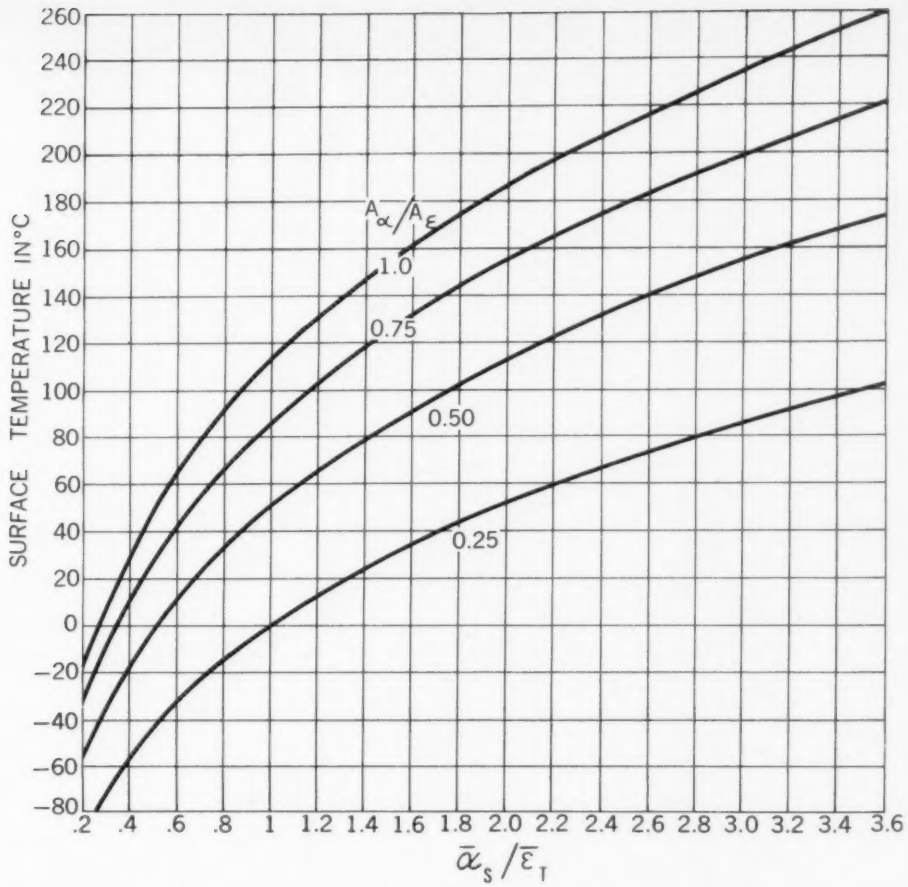

FIG. 6—Graphical solution of equation [6] for $f = 0.10$ and $C_1 = 1400$ wm^{-2}.

tween various parts of the body of which the element under consideration is part. The effect of other celestial bodies has also been neglected.

For orbits around the sun, the following simplified equation can be used:

$$T = \left[\frac{1-f}{\sigma}\left(\frac{A_\alpha}{A_\epsilon}\right)_s\left(\frac{\bar{\alpha}_S}{\bar{\epsilon}_T}\right)C_1\right]^{1/4} \qquad [6]$$

Equation [6] has been solved for the case of $f = 0.10$ and $C_1 = 1400$ wm^{-2}, and is shown in Fig. 6. It can be seen that for a flat oriented collector with radiation also from its back surface ($A_\alpha/A_\epsilon = 0.5$), and with negligible temperature difference between front and back surfaces, the determining ratio $\bar{\alpha}_S/\bar{\epsilon}_T$ should not be much larger than 1, otherwise the temperature will be too high for good cell efficiency.

To reduce the silicon solar cell temperature when the ratio A_α/A_ϵ as well as the orbit height are given, the ratio $\bar{\alpha}_S/\bar{\epsilon}_T$ must be decreased. This can be accomplished by either reducing $\bar{\alpha}_S$ or increasing $\bar{\epsilon}_T$, or doing both.

GLASS FILTERS

The reduction in $\bar{\alpha}_S$ without decreasing the power output of the solar cell, can be achieved by a coating which reflects radiation of wave length below 0.45 microns and between 1.1 and 3 microns. These regions represent about 16% and 22% respectively, of the total solar radiation in space.[15] This "ideal coating," which would have unit reflectance in these regions and unit emittance elsewhere, would yield a $\bar{\alpha}_S/\bar{\epsilon}_T$ value of about 0.6/1.0, or 0.6.

To obtain low values of $\bar{\alpha}_S$, research is being conducted by various establishments to develop band pass filters having the reflective characteristics described in the preceding paragraph, and considerable success has been achieved. For instance, interference film filters can be supplied which are vacuum deposited on to glass cover slides and which will reflect the ultraviolet end of the spectrum. The cut-off point can be specified. The filters* illustrated by curve C of Fig. 7, and by Fig. 11A, have a 50% transmittance at 0.45 microns;

* Optical Coating Laboratory Inc., Santa Rosa, Calif.

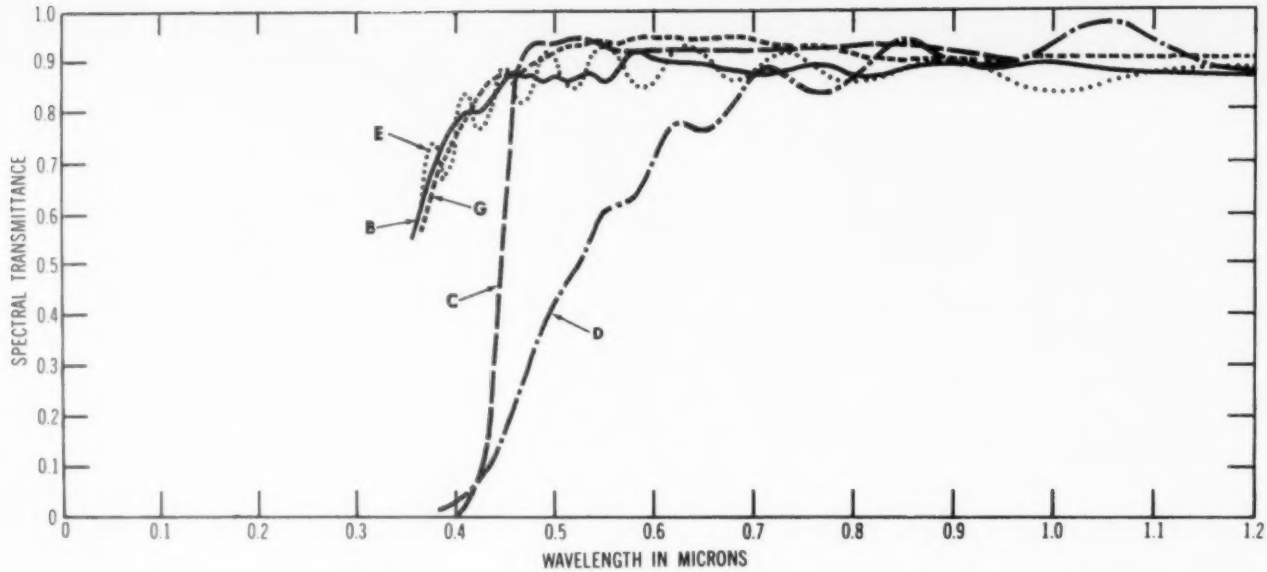

FIG. 7—Spectral transmittance below 1.2 microns for various coatings. (See Table II for description.)

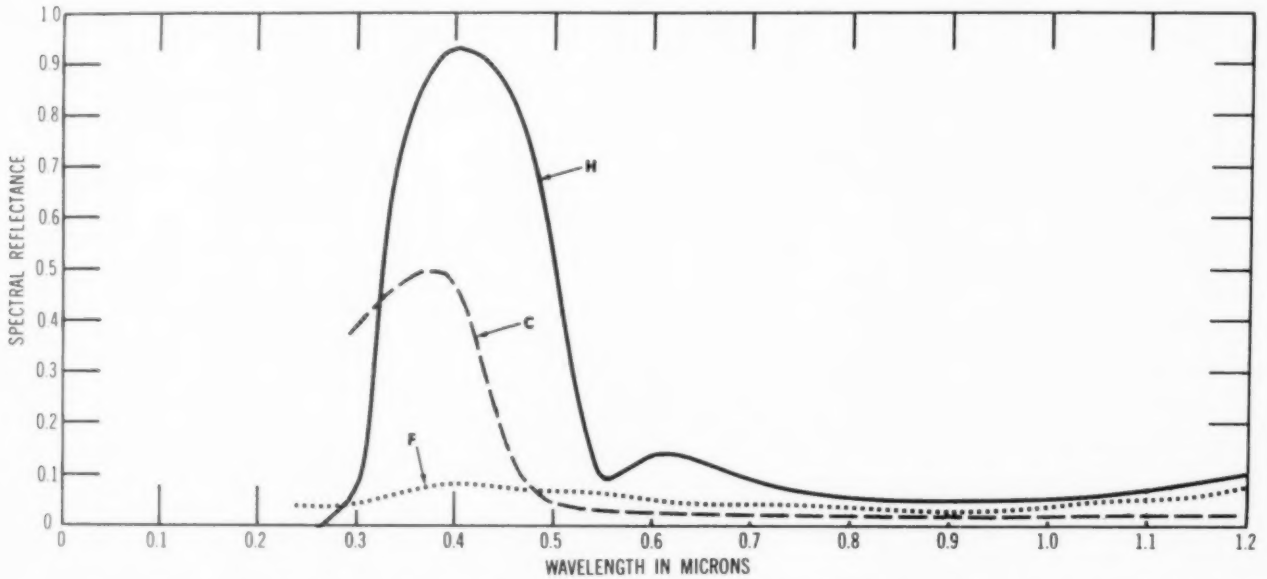

FIG. 8—Spectral reflectance below 1.2 microns for various solar cell surfaces. (See Table II for description.)

below 0.4 microns the transmittance is negligible, part of which, however, is an actual absorption loss. Since glass reflects at least 4 per cent of sunlight between 0.5 and 1.2 microns, the glass covers can also be provided with an unreflecting film to reduce the reflection coefficient in this spectral region to about 2 per cent.

From the spectral reflectance data shown in Fig. 8, curve *C*, and the Johnson curve for solar radiation (Fig. 1), the average absorptance for a solar cell provided with one of these filter glass covers has been calculated by Equation [2] to be about 0.90.

Newly developed interference filters are now available[16-17] that reflect sunlight on each side of the spectrally sensitive region of the solar cell (Fig. 1), that is, in the ultraviolet and near-infrared. Fig. 11B for instance, illustrates the transmittance of a typical "blue-red reflector" made by the Optical Coating Laboratory.[16] Out of the 23% of the solar energy above 1.1 microns, this coating reflects about half. Spectral reflectance measurements are required on solar cells covered with these new filters to enable accurate calculations of average solar absorptance, $\bar{\alpha}_s$.

Efforts to increase the average total emittance have

VOL. 4 1960

been even more successful. Glass, which is transparent in the response region of the silicon solar cell, yields a high value of emittance in the infrared.[18] Hence, the most widely used method has been to cement thin glass covers (thickness 0.006 inches or less) to the top cell surface using thin transparent organic cements (resins). An ultraviolet reflecting filter (Fig. 11A), is applied to the under surface of the glass to prevent ultraviolet degradation of the cement and to reduce the average solar absorptance, as described in the preceding paragraph.

By using the filter glass cover, the average total emittance (calculated by Equation [4]) of the solar cell between 0 and 150 C, is increased to 0.85–0.90, as shown in Fig. 5, curve *C*.

DIRECT COATINGS

Another method being investigated utilizes inorganic coatings directly deposited in vacuum on the solar cell.[16] It is known that silicon monoxide has low infrared reflectance, but solar cells coated with silicon monoxide have shown a severe decrease in conversion efficiency, because of poor transmittance in the visible region. (See Fig. 7, curve *D*, for instance.)

Some preliminary success has been achieved, however, with silicon oxides, SiO_x, applied by special

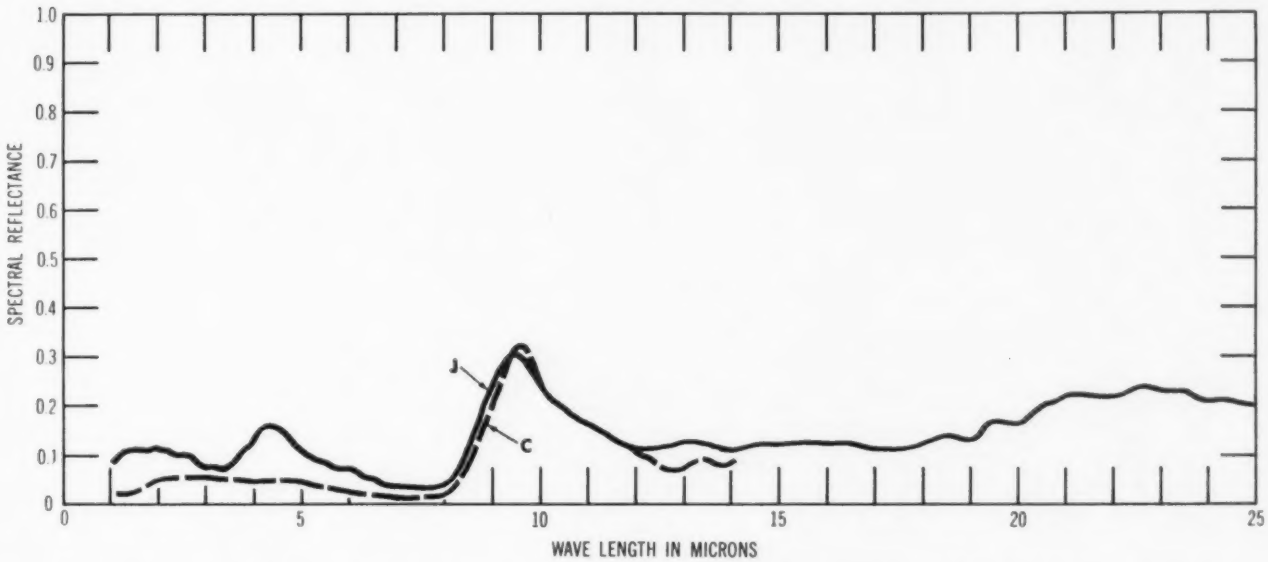

FIG. 9—Spectral reflectance above 1 micron for silicon solar cells with glass covers. (See Table II for description.)

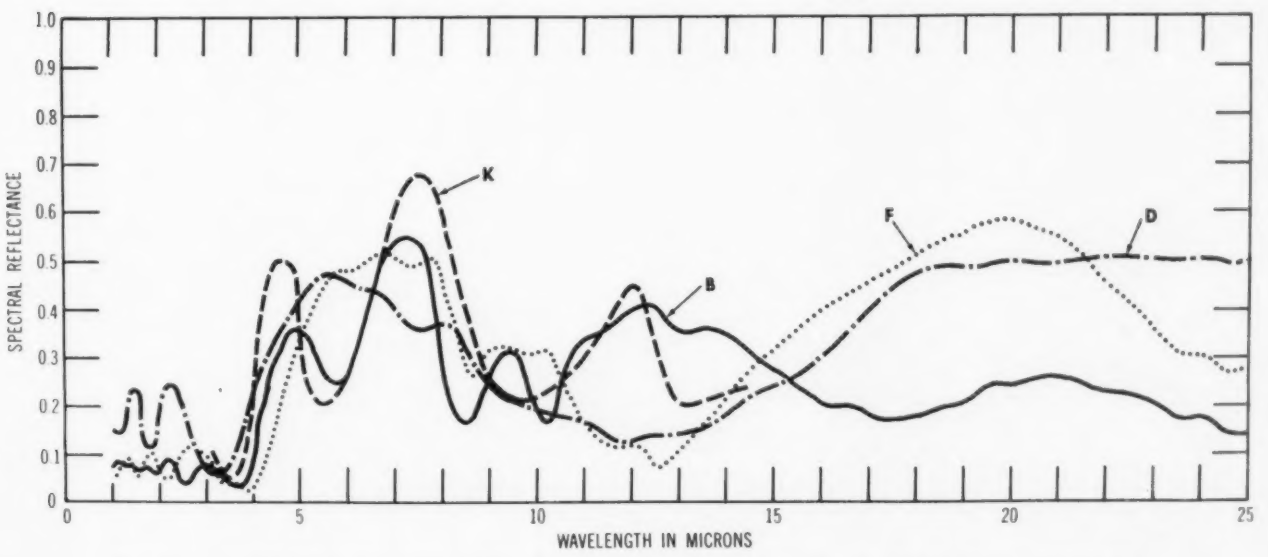

FIG. 10—Spectral reflectance above 1 micron for various solar cell surfaces. (See Table II for description.)

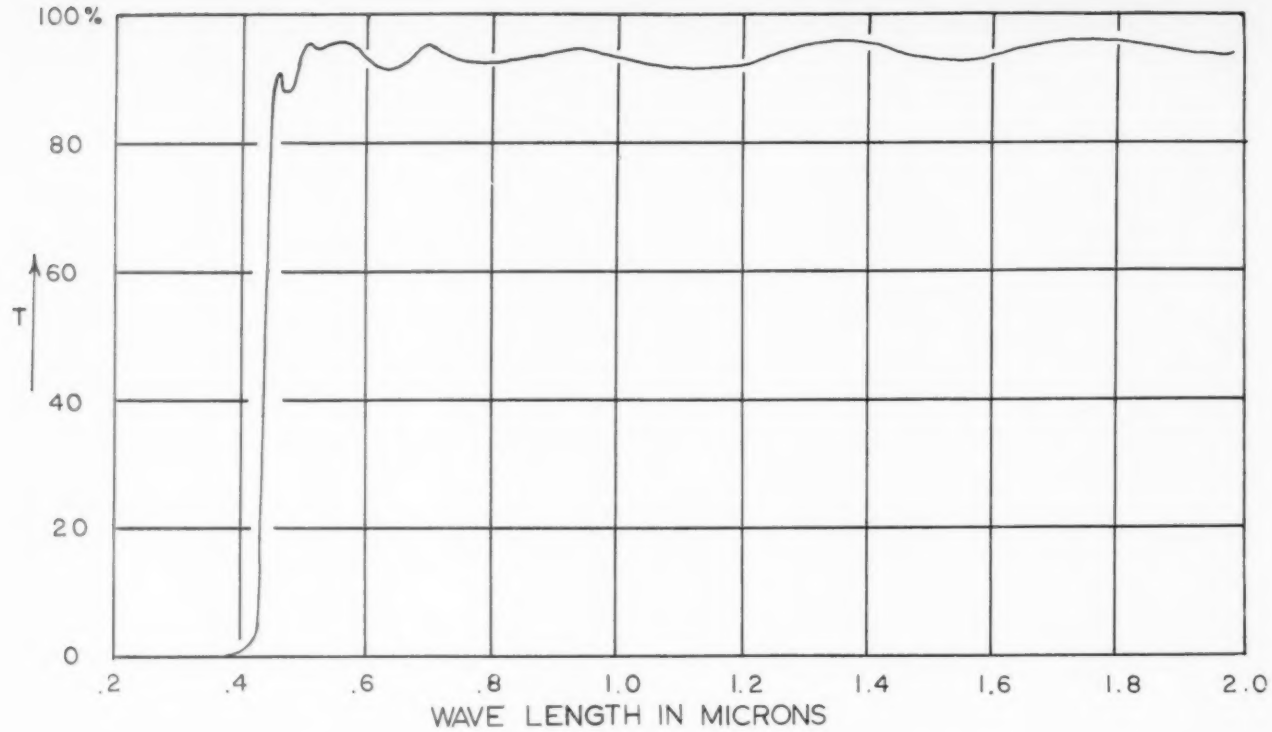

FIG. 11(a)

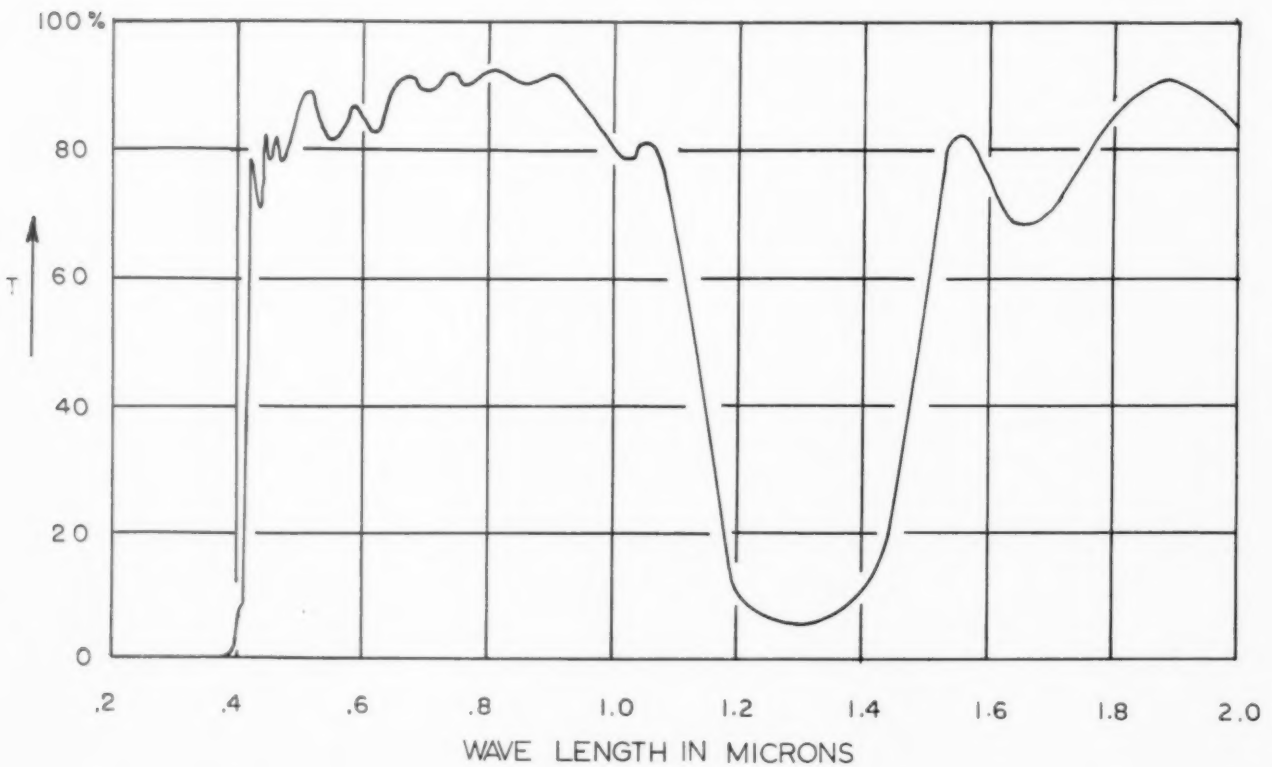

FIG. 11(b)

FIG. 11—Transmittance of glass cover with MgF_2 unreflecting film on one side and interference filter coating on the other side. (a) 16-layer ultraviolet reflector; (b) 41-layer ultraviolet-infrared reflector. (Courtesy of Optical Coating Laboratory.[16])

VOL. 4 1960

methods. [19, 20] These direct coatings offer some advantages over glass covers with respect to decreased weight and costs.

Figs. 8 and 10 illustrate the spectral reflectance for various direct coatings. For coating *B*, Table II, calculations indicate the average solar absorptance to be about 0.93, and the average total emittance (0–150 C) to be 0.75–0.72. The latter is illustrated in Fig. 5, curve *B*.

Although the emittance is not quite as high as with glass, the improvement over the uncovered cell is quite significant. Higher values of emittance can be obtained with thicker oxide films but only at the expense of impaired adhesion and transparency of the coating.

The experience obtained so far, therefore, indicates that it is possible to prepare adherent and durable silicon oxide coatings with little if any reduction in cell output. Table I, for instance, illustrates the average reduction in optimum power output obtained with a number of cells coated with some of the silicon oxide films shown in Fig. 10.

The composition[20] of the silicon oxide seems to be intermediate between SiO and SiO_2, and is probably Si_2O_3, with a refractive index of about 1.6. The transparency and adhesion of the coating depend to a large extent on the conditions of deposition, and it appears that solar cells with properly applied coatings can withstand severe environmental conditions, except of course, intense radiation. For instance, recent information[21, 22] indicates that quartz covers 0.070-inch thick are required to provide protection from an integrated electron flux of about $10^{15} e/cm^2$ at an energy of 800 Kev.

TABLE I

Coating	Physical Thickness	Average Reduction In Optimum Power
	microns	
(*B*) Si_2O_3	2.6	3%
(*E*) Si_2O_3	1.3	2%
(*F*) $Si_2O_3 + MgF_2$	1.3	1%

TABLE II

A. Non-coated, boron-doped, silicon solar cell.
B. Direct coating of Si_2O_3, approximately 2.6 microns physical thickness.
C. Glass cover having an ultraviolet filter on one side and a MgF_2 unreflecting film on the other.
D. Direct coating of silicon monoxide SiO, approximately 1.1 microns physical thickness.
E. Direct coating of Si_2O_3, approximately 1.3 microns physical thickness.
F. Same as (*E*) but with an unreflecting film of MgF_2.
G. Same as (*B*) but with an unreflecting film of MgF_2.
H. Glass cover with ultraviolet filter.
J. Glass cover.
K. Direct coating of silicon monoxide, 1.9 microns physical thickness.[14]

Table II describes the code used to identify the coatings and surfaces illustrated in the various figures. Transmittance values refer to the surfaces on 0.006-inch glass, whereas reflectance values refer to the coatings applied to the solar cell.

SUMMARY OF RESULTS

Average solar absorptance and average total emittance—which determine cell temperature and, consequently, power output of solar cells—have been calculated from measurements to 25 microns of the spectral reflectance of various solar cell surfaces. For bare solar cells, the absorptance and the emittance (0–150 C) are, respectively 0.93, and 0.35–0.40; for cells with ultraviolet reflecting glass cover, the values are 0.90 or less, and 0.85–0.90; and for cells directly coated with a special silicon oxide film, they are about 0.93, and 0.75–0.72.

REFERENCES

1. Chapin, D. M., Fuller, C. S., and Pearson, G. L., "A New Silicon *p-n* Junction Photocell for Converting Solar Radiation into Electrical Power," *J. Appl. Phys.* **25,** 676 (1954).
2. Escoffery, C. A., "Photovoltaic Conversion of Solar Energy," *Proceedings of the American Power Conference*, **22,** March 1960. (Illinois Institute of Technology, Chicago). Also to be published in *Semiconductor Products* **3** (*12*), December 1960.
3. Loferski, J. J., "Theoretical Considerations Governing the Choice of the Optimum Semiconductor for Photovoltaic Solar Energy Conversion," *J. Appl. Phys.* **27,** 777 (1956).
4. Tauc, Jan, "Generation of an EMF in Semiconductors with Non-Equilibrium Current Carrier Concentrations," *Rev. Mod. Phys.* **29,** 308 (1957).
5. Rappaport, P., "The Photovoltaic Effect and its Utilization," *RCA Review* **20,** 373, (1959); also *Solar Energy* **3,** December (1959).
6. Wolf, M., "Limitations and Possibilities for Improvement of Photovoltaic Solar Energy Converters," *Proc. IRE*, **48,** 1246 (1960).
7. Queisser, Hans J., and Shockley, W., "Some Theoretical Aspects of the Physics of Solar Cells," Conf. Paper 1293-60, *Am. Rocket Soc.* Space Power Systems Conf., Santa Monica, Calif., Sept. 27–30, 1960.
8. Jacob, Max, *Heat Transfer*, (John Wiley & Sons, New York), **1** (1949) and **2** (1957).
9. Dunkle, R. V., "Spectral Reflectance Measurements," in *Surface Effects in Space Craft Materials*, F. J. Clauss, Editor (John Wiley and Sons, New York, 1960), p. 157.
10. Fan, H. Y., and Becker, M., "Infrared Optical Properties of Silicon and Germanium," in *Semiconducting Materials*, H. K. Henisch, Editor, (Butterworth Publishing Co., London, 1951), p. 132.
11. Pfann, W. G., and van Roosbroeck, W., "Radioactive and Photoelectric *p-n* Junction Power Sources," *J. Appl. Phys.* **25,** 1422 (1954).
12. Spitzer, W. G., and Fan, H. Y., "Determination of Optical Constants and Carrier Effective Mass of Semiconductors," *Phys. Rev.* **106,** 882 (1957).
13. Philipp, H. R., and Taft, E. A., "Optical Constants of Silicon in the Region 1 to 10 ev," *Phys. Rev.* **120,** 37 (1960).
14. Hall, J. F., Jr., "Optical Properties of a Highly Boron-Doped Silicon Surface," *J. Opt. Soc. Am.* **50,** 633 1960. We are indebted to Dr. Hall for personal comments.
15. Johnson, F. S., "The Solar Constant," *J. Meteorology* **1,** 431, (1954).
16. Thelen, Alfred, "The Use of Vacuum Deposited Coatings to Improve the Conversion Efficiency of Silicon Solar Cells in Space," Conf. Paper 1298-60, *Am. Rocket Soc.* Space Power Systems Conf., Santa Monica, Calif., Sept. 27–30, 1960.

17. Evans, W. H., Mann, A. E., and Wright, W. V., Jr., "Solar Panel Design Considerations," Conf. Paper 1296-60, *Am. Rocket Soc.* Space Power Systems Conf., Santa Monica, Calif., Sept. 27–30, 1960.
18. McMahon, H. O., "Thermal Radiation Characteristics of Some Glasses," *J. Am. Ceramic Soc.* **34,** 91, (1951).
19. Auwarter, M., U. S. Patent 2,920,002, issued Jan. 5, 1960.
20. Cremer, E. C., Kraus, Th., and Ritter, E., "Uber das Absorptionsvermögen dünner Siliziumoxydschichten in Abhängigkeit von Oxydationsgrad," *Z. Elektrochemie,* **62,** 939 (1958). We are indebted to Dr. Thelen of the Optical Coating Laboratory, Santa Rosa, Calif., for comments regarding the characteristics of silicon oxides.
21. Fraser, J. C., Tompkins, D, H., and Valachovic, B., "Electron Irradiation of Silicon Solar Cells," Conf. Paper 60-1094, *AIEE* Pacific General Meeting, San Diego, Calif., Aug. 8–16, 1960.
22. Downing, R. G., "Electron Bombardment of Silicon Solar Cells," Conf. Paper 1294-60, *Am. Rocket Soc.* Space Power Systems Conf. Santa Monica, Calif., Sept. 27–30, 1960.

VOL.
4
1960

Solar Space Heating and Air Conditioning in the Thomason Home

Harry E. Thomason

Civilian Patent Advisor, Army Signal Corps, Pentagon, Washington, D. C.

The problems of successful solar space heating are many and varied. The scientist and engineer who starts out merely to heat his home by solar energy, with presently known apparatus and materials, faces a very difficult situation because the amount of heat energy received per square foot of surface per heating season is quite low, and the cost of previous efficient solar heat collectors has been high. Further problems are involved because the solar input occurs only about 6 hrs out of 24, and because many cloudy days per season plague the solar scientist. This paper reports the author's attempts to solve these difficult problems of solar space heating and cooling.

Heat Collector

The heat collecting device itself should intercept as much sunlight as possible, should be as low in cost and long-lived as possible, and should be as efficient in trapping solar energy as possible. Freezing and bursting must be avoided.

Heat Storage

If a heat collecting device as set forth above can be devised, then a tremendous surge of heat will be available during about 6 hrs on the sunny day, which, under "average" conditions, will be followed by a cloudy day. Thus, the surge of heat collected during a six hr period must be stored away for use during a 48 hr period. And, what is even worse, there may be several sunny days where a six hr surge of heat must be stored away each 24 hr period; then five to eight cloudy days may follow when no solar heat is available. Thus, two additional problems are apparent: provision must be made to absorb and store the tremendous six hr surge of heat rapidly, and provision must be made to store the greatest amount of heat for long cloudy spells. If these goals can be achieved, then the size of auxiliary heat required will be minimized but only if the following problems can also be resolved.

Getting the Heat Out of Storage

The heat storage apparatus must be capable of giving up large quantities of heat to heat the home when the weather is bitter cold, must be capable of minimizing undesirable heat losses, and must be capable of automatic heat release by simple low-cost thermostatically controlled apparatus. The importance of this requirement cannot be overemphasized. For example, it is easy to store significant quantities of heat in Glauber's salt at temperatures near 95 F, but it is very difficult to get this stored heat back out of the salt fast enough to keep the home warm on a bitter cold night. There is little comfort in knowing that you have a great reserve of heat stored away if you cannot get it out when you need it. Here again, low cost, simplicity and long-lived apparatus is essential.

Combining with Standby Heat Apparatus

A simple low-cost control system is necessary, and the system should be combinable with conventional but low-cost standby heating apparatus for the one exceedingly bitter cold winter in fifty, or for emergencies.

There are differences of opinion as to whether the auxiliary standby heating system should be large enough to do the entire job of heating irrespective of the solar heat. In some installations a smaller standby system is less expensive to purchase and repair. However, where oil is used for auxiliary heat, as a practical matter little can be gained by using a special furnace of low capacity. The chimney, the oil drum, and the controls are substantially the same as to cost, space requirements, and installation costs. Inasmuch as mass production of oil furnaces of a capacity of approximately 100,000 Btu per hr has lowered the cost, and repair parts are so readily available, there appears to be little advantage in installing a special furnace of 25,000 Btu per hr capacity which would cost substantially the same but might not be capable of heating the home under severe conditions if the solar system were temporarily incapacitated, such as by burning out of a pump motor or control which could not be replaced for a day or two.

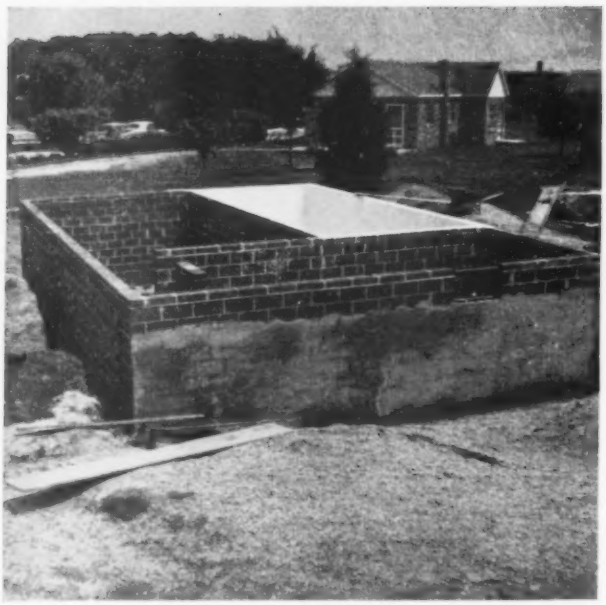

1. Foundation walls with heat bin, basement at left and recreation room and bomb shelter in foreground.

2. Applying insulation base for heat collector.

Also, it is always possible that the coldest weather ever recorded for a certain area may come on the heels of 10 cloudy days when the solar heat reserve is substantially depleted.

Thus, it is believed worthwhile to have the standby heating apparatus capable of taking over the entire heating load if necessary and to have it designed to operate with the solar system by the most simple and least expensive switchover mechanism possible. The standby heat apparatus should be of standard construction to reduce the likelihood of expensive maintenance.

Now assuming the builder-inventor has successfully met the above requirements, he is now in position to heat his home most of the time and save perhaps $100 to $200 per year for fuel. His apparatus is idle about five to six warm months of the year and working at only half capacity for another three or four months which are only moderately cold. But there are additional savings which may be achieved by the utilization of the apparatus during the idle time.

Air Conditioning, Domestic Water Heating

The solar heating system can be made more valuable if domestic water heating and summer cooling can be incorporated. A saving of $50 to $125 a year can be realized on hot water alone. If central air conditioning can be worked in without use of expensive heat pumps (which require 2 to 5 hp motors) a further sizable saving in electricity can be realized. Equally important, the apparatus now becomes usable the year-around. Also, inasmuch as heat-pump type central air conditioning costs some $1,000 for the original installation, the *original cost* of a solar heated and air conditioned home may begin to approach that of a conventional home, and true savings for fuel and electricity will result *if* all of the above factors can be met.

Swimming Pools, Greenhouses

Further, if the solar scientist can approach the requirements set forth herein above, he can look around for further uses for his surplus free solar heat which is available at times. For example, he can use surplus heat for a swimming pool in the autumn and spring and can thus double the season for swimming and make the expensive pool itself much more valuable. Also, he can heat a greenhouse to lengthen the growing season. His system is now not only paying off economically, but is providing comforts and luxuries which cannot be afforded by the ordinary working man.

Meeting the Problems

To make the solar collector itself worthwhile it must be low in cost. Even if the collector is turned directly into the sun it can intercept a maximum of only about 300 to 350 Btu/sq ft/hr. If the collector is movable to track the sun, the apparatus is expensive. If it is fixed, the solar energy intercepted will be only about three to four Btu/sq ft/min, average, for only about six hours, only on sunny days. When it is considered that a gallon of oil gives about 100,000 Btu for about 15¢, then the necessity for low cost solar heat collector construction becomes obvious.

VOL.
4
1960

Lowering Collector Costs

How can the cost be lowered? If specialized construction is used the cost will go up, at least for several years until mass production and mass sales of the specialized construction can be achieved. But, if conventional materials which are readily available at low cost can be used, then one can start out with low cost solar apparatus. The construction should be fast, simple and easy to assemble by semi-skilled workmen. Examples of low cost materials which are readily available are insulation at about 5¢ to 10¢ per square foot, conventional metal roofing at about 10¢ to 15¢ per sq ft, glass or transparent plastic at about 12¢ to 20¢ per sq ft.

The Thomason Collector

The basic materials set out above have been combined to produce a heat collector construction on the Thomason solar heated home at a cost of only about $1 per sq ft, (patents pending). Conventional roofing rafters form the supporting structure for the collector. A reflective insulating base is covered by corrugated sheet metal which is treated on its upper surface to make it black. A transparent plastic cover is immediately above the corrugated metal and ordinary window glass is supported about 1 in. above the plastic. The corrugations run down the incline and a distributor manifold brings hundreds of small streams of cold water into the various valleys. As it runs down the hot black metal surface, the water is heated. The hundreds of small streams of hot water are collected into one large stream at the bottom of the collector, and the hot water flows to the heat storage bin to heat domestic water and to heat the home.

Performance Data—Heat Collector

Solar heat collection varies widely from a minimum on a dark cloudy day to a maximum on a clear, calm day with a minimum of haze and with snow on the ground to intensify heat and light intercepted by the collector. Of course, if the day is warm, then less heat will be lost from the collector—though the collector output does not drop very greatly during cold days. Thus, it is very impressive to note the unexpected collector output on a cold bright sunny day. However, for heating pool water to about 80 F a reasonable amount of heat can be trapped *even on a dark cloudy day*, and this is a fact which is very surprising to most people. Typical performance data on the collector is as follows for a sunny day.

On 8 December and 9 December 1959, near the shortest day of the year, the weather was mostly sunny, with a low of 29 F each night. Mr. Torrence H. MacDonald of the U. S. Weather Bureau made on-the-spot checks at 12:40 PM on the 9th and reported the solar input at 4.65 Btu per sq ft per min and reflection from the collector at 15%. Rough measurements each day were approximately as follows. Flow rate, 7.15 gpm; temperature rise from 92 F to 119 F. The net heat collecting area of the solar heat trap is approximately 700 sq ft after deducting for glass supporting members (overall dimensions are 38′ x 22′). Thus, the rate of heat collection was approximately 2.2 Btu per sq ft per min and efficiency was approximately 47%.

3. Applying corrugated sheet metal, to be painted black.

4. Finished home-view from street.

For heating cold city water from 51 F to a swimming pool temperature of 83 F at a rate of approximately 10 gpm the rate of heat collection was more than 150,000 Btu per hr or approximately 3.6 Btu per sq ft per min with an efficiency of approximately 78%.

The rough tests were conducted as follows. Mr. MacDonald made his checks on solar input and heat collector reflection with a pyrheliometer. Readings of the temperature of the water going to the collector were taken from a thermometer installed in the supply line to the collector. A "five gallon" bucket, graduated to indicate one to five gal was used to catch five gal of water from the collector outlet three different times for each test and the timed results were averaged to determine the flow rate. The temperature of the water in the bucket was checked as each five gal was caught. (Water was circulated through the collector for some three and one half hours prior to the testing, thus eliminating any possibility of abnormal readings due to heat build-up prior to the testing.)

Although the author did not have an expensive pyrheliometer to check solar input, the author and his wife made temperature readings and checks on flow rate all during the winter. On bright sunny days the temperature rise between collector input and output was very similar to the readings taken on 9 December 1959. However, when snow was on the ground the temperature rise was several degrees higher than it was on 9 December. Also, when the temperature of the water going to the collector was down to 70 F to 80 F, such as occurs at the end of a few cloudy days, then the temperature rise was considerably greater, and efficiency went up far above the 47% indicated previously. December 9, 1959, was about as bright and clear a day as Washington winters provide.

The temperature rise in the 70 F to 100 F range was consistently higher on days not as bright as this. Therefore, the efficiency was much higher, indicated to be approximately 60% in the 70 F to 100 F range. The author could not detect any appreciable lowering of efficiency during the winter, although there may have been some small change.

The low cost, high efficiency construction described is possible because it is made of less expensive materials which requires less expensive labor and because the design absorbs and transmits heat rapidly. Carpenters and laborers can handle the commercially available corrugated sheet metal, wood, and insulation at a much lower square foot cost than the cost of the more specialized labor incident to the installation involved with tube-in-sheet collectors. In tube-in-sheet metal collectors the cost may run as high as $2.50 per sq ft in contrast to the $1.00 per sq ft achieved by the corrugated sheet metal design. Expensive copper tubing with expensive copper fittings are soldered to expensive copper sheeting with expensive solder by expensive labor. In the copper tube construction, the tubes are usually limited to about a six inch spacing to keep the cost from running even higher, thus limiting the amount of heat which can be carried away by the circulating fluid in the tubes. With the six-inch tube spacing heat may travel a maximum of 3 in. to be transferred to the water within the tubes. This usually results in such a build up of temperature at the mid point between the tubes that much heat is lost by reradiation to the surrounding atmosphere.

The corrugated construction on the other hand, in addition to being basically cheaper because of the availability of materials, and construction labor, is more suitable for trapping heat since the valleys in the corrugated sheet metal are close enough together for most of the absorbed heat to be transferred into the water which at no time is more than $\frac{5}{8}$ in. away. Prior to the construction of the author's 700 sq ft collector using the corrugated material, there was some concern that its large size might involve unforeseen cost factors. Upon completion of the collector, however, it was found that its unit cost had dropped to about $1.00 per sq ft. In fact, both the unit cost and the efficiency had been improved from a previous 120 sq ft model at $1.50 per sq ft of the same general construction which had been tested on an earlier Thomason home.

VOL.
4
1960

Condensation

There was some concern that the condensation which might be expected to occur on the underside of the lower transparency would block entrance of sunlight and lower efficiency. This condensation, however, seems to have only a negligible effect on entrance of sunlight to the blackened surface. Upon close analysis it is found that the droplets of condensation form tiny magnifying lenses. The sunlight strikes the droplets and the rays are deflected toward the focal point of each drop. If the blackened sheet metal happens to be just far enough from the droplet to intercept the rays at the focal point, a hot spot occurs. If the rays are intercepted before or after the point of convergence, the rays are spread out and strike the blackened surface with more uniformity and less concentration. In either case the transmission through the transparency and condensed droplets is good, and efficiency of the entire collector remains high. Mr. Torrence H. MacDonald of the U. S. Weather Bureau at Washington took on-the-spot readings and reported that only 15% of the sunlight was being reflected away from the collector. Under some conditions, as in the heating of the swimming pool water mentioned earlier, the efficiency of the collector itself is approximately 75% to 80%. Thus one may conclude that very little loss occurs from the condensation problem.

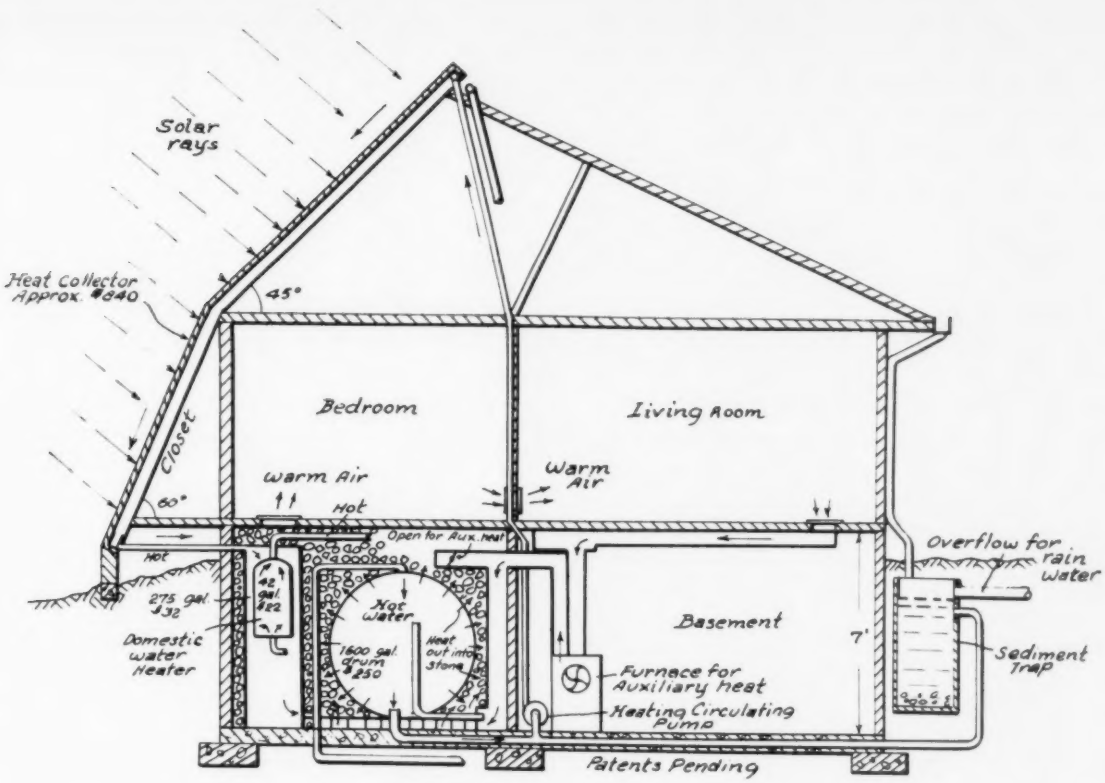

Winter Heating Cycle

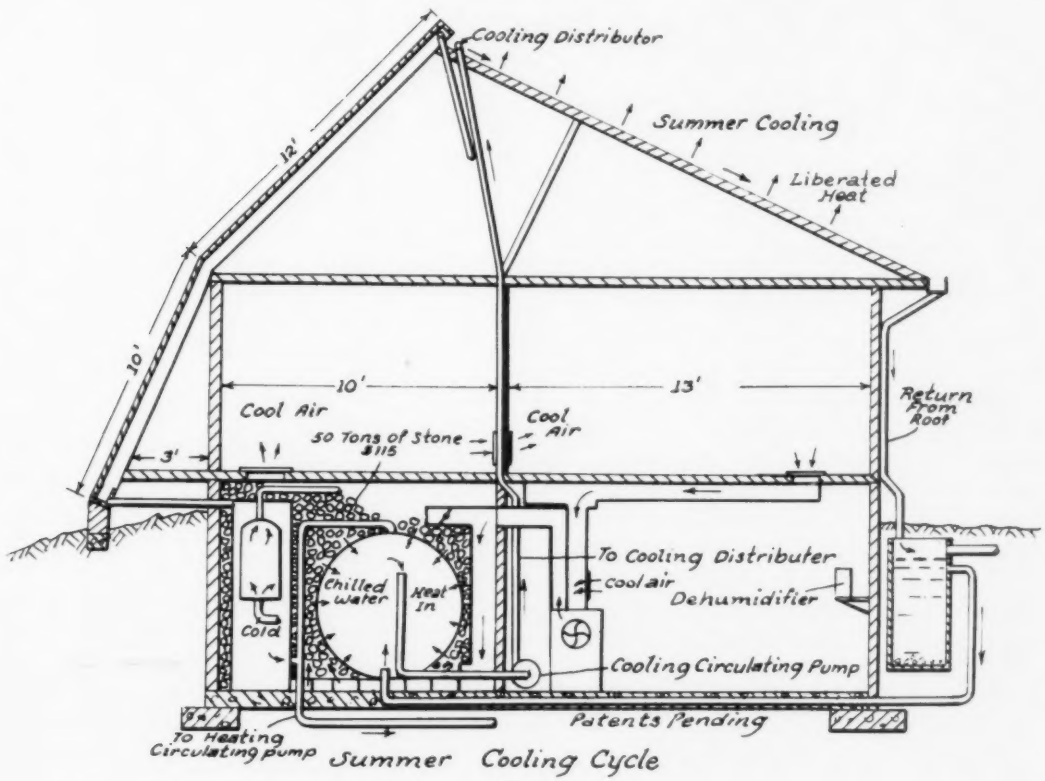

Summer Cooling Cycle

FIG. 5.

The sealing means for the glass on the 700 sq ft solar collector is fair. However, a new sealing means has been invented which should be much better, less expensive, and quicker and easier to install. Further details as to the several methods of sealing will be reported later.

Heat Storage Solution

One major problem is solved once a low-cost, simple, highly efficient heat collector has been devised. However, an equally difficult solution to the heat storage problem still remains to be found. How does one go about devising a storage system which has adequate capacity, which is inexpensive, simple, long-lived and from which one can withdraw heat by simple automatic controls in large quantities for bitter cold nights? Can one also devise a system of storage which may be reversed during the summer for "cold" storage? If so, then the storage apparatus is of greater value because it is usable the year around, and it can be used to stabilize home temperatures during variable spring and autumn weather.

The heat storage apparatus reported here (patents pending) is placed in a bin which occupies about one third of the floor space of the basement. This bin is 10 ft wide, 25 ft long and 7 ft deep. It contains a 1600 gal drum 4 ft in diam by 17 ft long which cost $250. The drum has a manhole for access to the interior. The bin also contains a domestic water preheater assembly, to be described later, and 50 tons of fist size stone at a cost of $115.

Preparation of the air-tight, insulated bin is simple and inexpensive. The foundation walls of the house and a wall beneath the center beam of the house form the heat bin walls at practically no added cost. These walls of building blocks are waterproofed outside in the conventional way and are painted inside with a paste made of ordinary cement mortar and water to seal cracks. A coating of white cement and lime was painted on, all at very low cost—about $6 for mortar and white cement for both coats. (A coating of reflective metallic paint would be of some value in reducing heat losses if added to or substituted for the white paint.) The bin is insulated with fiberglass or rockwool. Strips of lumber 2 in. x 3 in. or 2 in. x 4 in. plus 1 in. undressed boards, prevent crushing of the insulation by the stone. In the bottom of the bin a simple air distributor system is constructed with only two man hours of work merely by placing building blocks to form a distributor manifold with ducts leading off therefrom formed by the holes in the building blocks. These blocks cover about two-thirds of the bin floor and lie on their sides with the holes aligned to form about 60 ducts leading from the distributor manifold. These blocks are quickly placed without mortar and are spaced about three-eights in. apart to provide hundreds of "perforations" in the ducts so that the air can circulate up through the stone and around the 1600 gal drum to be heated in the winter or cooled in the summer. It is important to note that the 50 tons of stone can be "dumped" into the bin at very little cost.

Ducts and registers are provided at the top of the heat bin to supply air to the various rooms of the house. Cold air registers provide for return of the air to the heat bin for reheating.

With this type of storage apparatus the water serves four functions and the stone serves in a double capacity. The water (1) serves as a heat transfer medium from the heat collector to the heat bin (and from the bin to the roof cooler for summertime), (2) serves to temporarily store the excessive surge of heat produced during the sunny day, (3) provides for a large amount of heat storage within the water itself between its lower useful level near 70 F and its upper level of about 135 F, and (4) the 1600 gal drum provides several hundred sq ft of heat exchange surface to get the heat into the air to be heated. The stone serves (1) as a heat storage medium of exceptional capacity and (2) provides an immense amount of heat exchange surface at very low cost.

With this arrangement of parts the heat from the bin can be used to a level below 80 F before auxiliary heat is needed, whereas it is difficult to get sufficient quantities of heat to warm the home on a cold windy night directly from water by conventional radiators even when the water is at a 100 F level. Also, the presently described apparatus is readily reversible for summertime "cold" storage.

Domestic Water Heating

Heating the domestic water supply by use of low cost simple apparatus presents somewhat of a problem inasmuch as domestic water must be heated the year around. Thus, during the summer one must produce heat for domestic water plus "cold" for air conditioning the home. To meet this requirement, this solar heated home has a 275 gal preheater drum insulated from the remainder of the heat bin. Inside of this drum there is a 42 gal tank into which domestic water to be heated flows. Heater water from the solar heat collector flows into the 275 gal drum and "bathes" the 42 gal tank in hot water to heat the fresh water inside. During the winter, the hot water from the 275 gal drum flows into the 1600 gal drum to heat the water therein and the stone thereabout for heating the home. A small circulating pump takes the cold water from the bottom of the 1600 gal drum and recirculates it through the heat collector for reheating.

During the summer the water from the 275 gal preheater drum does not pass into the 1600 gal drum but passes directly to the circulating pump and back to the heat collector until the water in the 275 gal drum is hot.

VOL.
4
1960

Thus, the preheater assembly, which is made up mainly of a $32 drum and a $20 tank, is usable the year around to cut electric bills for domestic water heating some $5 to $10 per month. Inasmuch as domestic water for clothes washing, baths, dishwashing, etc., for the author's family of seven, is heated mainly by the sun, the resultant saving in electricity is about 250 to 400 kw per month, even after allowance is made for electricity to operate the small circulating pump for the heat collector. Even though the family's use of hot water and electrical appliances has increased, the electric bill has decreased considerably for the new home. A total of 275 gal of hot water is inside the preheater, 42 gal in the small tank being hot for immediate use. A small electric water heater is provided to boost the domestic water temperature a few degrees during long cloudy spells, but even then the preheater warms the water considerably before it passes into the electric heater. The solar water heater heats the water to about 140 F to 150 F for summer and about 125 F to 135 F during the winter. A thermostat cuts the circulating pump off when the preheater temperature reaches about 145 F to 150 F.

Summertime Cooling

During the hot summer months "coolness" is acquired from various sources and is stored. Water from the 1600 gal drum is circulated over the north roof of the house at night and the water is chilled due to radiation and evaporation. The chilled water in the 1600 gal drum, chills the stone. Then, next day when the home needs cooling, warm air in the home is circulated around the chilled drum of water and through the chilled stone to cool the home. Water lost due to evaporation from the roof is replenished by rain.

Additional cooling is obtained by circulating a portion of the air through the basement, the recreation room and bomb shelter. A small dehumidifier in the basement keeps this air dry on humid days. As this air mixes with the air circulating through the house the humidity is lowered. A kitchen exhaust fan removes excess heat from cooking.

During warm humid nights very little heat is liberated by way of the roof dissipator. Under these conditions the system draws upon stored "coolness" for cooling the home on hot afternoons.

Although we never have very low humidity in the Washington area, such as in our midwestern states, nevertheless the roof dissipator has chilled water in the 1600 gal drum at a rate of 25,700 Btu per hr on a cool summer night when the humidity was not excessive. This is substantially equivalent to three ordinary window air conditioners of the 1 hp class.

Air conditioning engineers recommend that the home temperature be lowered about 10 F to 15 F below hot outside temperatures. This home was cooled to about 8 F to 14 F below outside temperatures throughout the entire summer, the home being about 78 F to 82 F most of the day with a maximum of 85 F when the temperature outside was 98 F as registered by a thermometer bulb in the shade on the north side of the house. Bin temperatures usually run about 77 F to 81 F with the 1600 gal drum temperature being about 65 F to 70 F. To achieve this amount of cooling and dehumidifying only about one-fourth hp is used, and thus a considerable saving in electricity is evident. Obviously this cooling system would be more effective in areas where the nights are cooler and drier. The air conditioning system has been improved in our latest solar home just completed.

Stabilizing Effect of Heat Bin

The heat bin is valuable for storing heat during the winter and for storing "coolness" during the summer. In addition, the storage apparatus is extremely valuable in stabilizing home temperatures during variable spring and autumn weather. Under these conditions a cold blast of air from the north may plunge temperatures to 32 F one night and yet a hot blast from the south may raise the temperature to 95 F two days later. With this storage system neither solar heat nor "coolness" is stored for most of the spring and autumn. The bin is permitted to level off at about 75 F. If the nighttime temperature drops to 32 F the stone and water at 75 F keeps the home warm. If the daytime temperature rises to 95 F the stone and water at 75 F keeps the home cool.

Heat Bin Compared with Storage Battery

This heat bin is comparable to a storage battery of tremendous capacity. It stores heat as an electric battery stores electricity. However, the heat storage battery is peculiarly usable by "reverse charging" to provide "cold" storage for summertime. Additionally, it is valuable spring and fall for stabilizing home temperatures when the battery is "dead" (at 75 F).

During the winter, when the heat bin temperature is up to 110 F to 125 F we have a well charged battery which will heat the home for 7 to 10 cloudy days. During this time the bin temperature is lowered day-by-day when the sun does not shine to about 75 F to 78 F. If there is still no sun, then a little auxiliary heat is used (a total of $4.65 worth of oil was used for the entire winter). When the sun reappears the battery is recharged.

Temperatures in the home were thermostatically controlled and kept at 70 F to 72 F throughout five rooms and bath and were kept at about 65 F in the basement. During the earlier part of the winter the home temperature was permitted to drop to 65 F at night but this practice was discontinued in midwinter and the home kept at 70 F to 72 F day and night. The home has an electric range, TV, etc., and an electric

clothes dryer in the basement, vented to the outside, which is used only about two days per month. There is no fireplace to aid in heating the home. If the home temperature drops to 72 F a thermostat cuts the furnace blower in to extract stored solar heat from the heat bin. If the home temperature drops to, say 68 F, a second thermostat cuts the standby furnace in. (However, to be certain of the amount of time the furnace ran and the amount of fuel used, the furnace thermostat was operated manually when temperatures dropped to about 69 F.)

During the summer nights the bin temperature is lowered to about 72 F for the stone and 62 F for the drum of water, (these figures vary depending on conditions). This reversely charged chilled battery will absorb excess heat for a few days if necessary while the battery temperature rises. However, at night it is reversely charged with "coolness" to absorb the heat of the day.

During variable spring and autumn weather the Thomason heat battery goes "dead" at 75 F but becomes extremely valuable at this time because it can stabilize home temperatures during months of the year with practically no expenditure of power. Inasmuch as the "cold snaps" or hot spells are short lived, it is rare that either solar heating or cooling is required. During the 32 F cold snap the home is kept warmed to 70 F to 72 F by drawing on the heat stored at 75 F. During the 95 F hot spell the heat bin temperature is raised back to 75 F to 78 F while the home temperature is kept down to about 78 F to 80 F.

Thus it is apparent that the heat bin battery is of great value the year around, being charged for wintertime, reversely charged for summertime, and valuable as a dead battery for spring and autumn.

Getting the "Coolness" out of the Bin

It is well to recall at this point that the problem of getting the stored "coolness" out of the bin is similar to getting stored heat from it in the winter. The stone and drum of chilled water have such large surfaces of contact with the air flowing thereabouts that the home can be maintained within a few degrees of the bin temperature. Typical conditions for a hot summer afternoon are: Outside temp 95 F, home temp 83 F, bin temp 79 F, water temp 70 F.

Performance Data—Roof Cooler

The roof cooling apparatus liberates heat by three different principles under favorable conditions, (1) evaporation, (2) radiation, (3) contact with air cooler than the water.

It is found that the water on the north sloping roof flows slowly in an almost perfect thin sheet from top to bottom. The granules of sand in the asphalt shingles help to spread the water evenly and to retard the rate of flow. (It has been reported that the roof will last longer due to this daily dampening of the shingles, but at this point the author cannot detect any changes in the roofing upon which to base an opinion.)

Evaporative Cooling. When the relative humidity of the air is low, cooling due to evaporation is excellent. A slight breeze is also helpful for evaporative chilling of the water. However, in the Washington area the relative humidity is rarely at a low point, generally ranging from 60% to 90% at night. In areas of the world which have low humidity, evaporative cooling would be very good.

Radiation Cooling. When the sky is bright and clear, cooling by radiation is at a maximum. Due to the north sloping roof not being very steep, radiation to the clear sky can be very valuable in chilling the water flowing thereover. However, in the Washington area the sky is often overcast or hazy and unfavorable for radiation cooling.

Cooling by Air Contact. Periodically during the entire summer a "cool front" will move down from Canada and will lower outside air temperatures to 65 F, perhaps as low as 58 F. Under these conditions, the water in the 1600 gal drum may be up to say 73 F to 75 F from cooling the house on previous hot days. Thus, when the water is circulated over the north sloping roof and it comes into contact with the cool air, the chilling process is aided.

Specific Cooling Performance of Roof Cooler

On the night of 18 June 1960 the following data was taken to illustrate cooling capability of the cooling apparatus.

Time	°F to Roof	°F from Roof	Air Temp. °F	Humidity	Weather
10:30 PM	72	67	63	Approx. 65–75%	Clear, calm
11:00	71½	66½	62	Approx. 65–75%	Clear, calm
11:30	71	65	61	Approx. 65–75%	Clear, calm
05:00 AM	64	59	56	Approx. 65–75%	Clear, calm

The rate of flow was 5 gal in 37 sec, and the cooling was from 5 F to 6 F. This yields approximately 19,000 to 23,000 Btu of cooling per hour.

On the night of 14 July the rate of cooling was at 25,700 Btu per hr at the peak when the sky was overcast, but there was a breeze of about 15 mph. Outside air was at 68 F, water to the roof was at 73 F with a return temp of 65½ F and a flow rate of 5 gal in 41 sec. Humidity was about 65%.

It is to be noted that the relative humidity was quite high (68% at 11:30 PM according to the Washington Weather Bureau). Had it been lower, cooling would have been at a better rate.

During some nights the air temperature may remain high (about 75 F), the humidity high (about 95%), the

VOL. 4 1960

sky overcast, and the air still. Under such conditions the roof chiller is not used at all and dehumidified air from the basement is cooled by the "coolness" stored in the 50 tons of stone and 1600 gal of water. The temperature in this home has not exceeded 85 F, and it is generally kept to 82 F to 83 F, even when outside temperatures rise to 95 F to 98 F. Fortunately, even if outside temperatures go to 98 F at 5:00 PM they are back down to about 82 F by bedtime. Thus, cooling is generally required only about six to ten hours per day, some cool days requiring no cooling.

Typical home temperatures are represented as follows. In late August Washington had a hot spell. On August 26 when the official high was 93 F and the temperature in the shade on the north side of the home reached 96 F, the temperature inside reached a maximum of only 82 F, the humidity being lowered from 63% to 60% between 11:00 AM and 6:00 PM.

Cooling Apparatus Costs Practically Nothing

The heat bin, blower, ductwork, etc., are required for wintertime solar heating. To add summertime cooling to the apparatus costs very little, inasmuch as the same bin, stone, blower, ductwork, and such are used for cooling also. About all that is added is a circulating pump, a few controls, and an insignificant amount of plumbing. (Due to high humidity in the Washington area we also added a small $85 dehumidifier.) Thus, the added cost of installation of central air conditioning in the Thomason solar system is only approximately $150. And, only about one-fourth hp is used for circulating water at night and a one-fourth hp for the blower on the hot days. Thus, the electric bill was kept much lower than it would have been with conventional air conditioning.

Standby Heating

As was indicated previously, it is important that a standby heat source be provided to take care of possible emergencies and the added load in the one winter in fifty which is extremely severe and cloudy. In our system this was taken care of merely by using a conventional oil furnace. The outlet duct is provided with a bypass and an automatic damper therein which remains closed at all times except for a few hours during the winter when auxiliary heat is needed. For normal operation, summer or winter, the thermostatically controlled furnace blower and filter circulate the air throughout the home and filter it. Then, when auxiliary heat is needed the furnace cuts on. A few minutes later the damper in the bypass opens and the hot filtered air ceases to pass through the stone and goes directly to the hot air registers. When the home is warm enough the furnace cuts off and a few minutes later the blower cuts off and the damper closes.

Insulation

The home is not heavily insulated. The walls are of 8-in. cinder blocks, with ¾ in. of Rainbow stone outside, 1½ in. of glass wool insulation inside, and dry wall. The ceilings are of ordinary ceiling tile with only 3 in. of Fiberglas insulation. Storm windows and doors are used along with ordinary venetian blinds and Fiberglas draperies.

Further Savings Due to Solar System

But this simple low-cost system with its fuel savings for the winter, air conditioning in the summer, and domestic water heating the year around has other potentialities. During the spring and fall and at times during the winter the surplus heat received can be used for heating swimming pool water. It is not uncommon at the home to see five youngsters playing in their solar heated pool while snow covers the earth around them. Contrary to popular belief the 2,000 gal pool (usually containing about 1200 gal of solar heated water) remains warm for many hours after being filled. The pool itself is of unusual low-cost design, but the details of its construction will not be discussed for the present.

Or one might use the surplus heat for a greenhouse. Details for heating a greenhouse with some of the surplus heat from the solar heated home have been worked out, but this, too, is beyond the scope of the present paper.

Costs of the Solar System

The three-bedroom Thomason home cost only $13,000. Altogether the house has five rooms, a bath, a utility room, a recreation room, a basement, and a bomb shelter.

The approximate costs of the heating and cooling system are as follows.

1. Solar heat collector	$840
2. Standby furnace	250
3. 1600 gal tank	250
4. Stone	115
5. Pumps, controls, etc.	150
6. Miscellaneous (insulation, distributor ducts, etc.)	200
7. Solar domestic water heater	50
8. Auxiliary water heater	50
9. Dehumidifier	85
10. Costs of labor	500
Total, approximately	$2490

It is likely that the solar heating and air conditioning system in a new home, now completed, will be cheaper and more efficient than the one here described. After thorough testing of the new system, if the results come up to expectations a limited number of licenses will be granted for the improved design.

Survey of Electron Transfer Spectra of Inorganic Ions*

Rudolph J. Marcus

Chemistry Department, Stanford Research Institute, Menlo Park, California

The literature was searched for electron transfer spectra of inorganic ions. These are reported, together with the chemical evidence of light-induced electron transfer and with thermodynamic data needed for interpretation of the spectra.

The portion of the absorption spectrum of an ion, molecule, or molecular complex which can be ascribed to transfer of an electron to or from the absorbing species is termed the electron transfer spectrum of that species. This subject was first reviewed by Rabinowitch,[1] whose paper still possesses current significance in the field, and more recently by other workers.[2, 3] The discovery of the electron transfer spectra of organic complexes and of organic-inorganic complexes by Benesi and Hildebrand[4] has expanded the field considerably. A considerable amount of work is being done on the electron transfer spectra of such complexes. In view of our interest in assessing the possibility of inorganic photosynthesis, however, we have limited our survey to consideration of the electron transfer spectra of inorganic ions.

This survey now contains the absorption peaks of 70 ionic species which have been recorded in the literature as electron transfer spectra. Of these, most are reductive spectra (Table I) which are due to electron transfers from various ligands to the central ion of a complex ionic species; for example

$$HgCl_4^{-2} \overset{h\nu}{\rightleftharpoons} [Hg^{+}Cl_4^{-3}] \rightarrow \text{products.} \qquad [1]$$

When the electron transfers from a water molecule or hydroxyl group to the central ion, hydroxyl radicals are formed initially with the ultimate formation of oxygen; for example[5]

$$Fe^{+3}\,(aq) \overset{h\nu}{\rightleftharpoons} [Fe^{+2}\cdot H_2O^{+}] \rightarrow Fe^{+2} + H^{+} + OH \rightarrow \text{products.} \qquad [2]$$

The remainder of the bibliography contains oxidative spectra (Table II) consisting of two well defined groups. Transition element ions react in acid solution to form hydrogen:

$$V^{+2} + H^{+} \xrightarrow{h\nu} V^{+3} + \tfrac{1}{2}\,H_2, \qquad [3]$$

and halide ions form the corresponding halogen:

$$I^{-} + H^{+} \xrightarrow{h\nu} \tfrac{1}{2}\,I_2 + \tfrac{1}{2}\,H_2. \qquad [4]$$

The electron acceptor always appears to be the hydrogen ion in the oxidative electron transfer spectra of inorganic ions. The proper combination of these two kinds of electron phototransfer reactions results in the decomposition of water into oxygen and hydrogen.[27] If the absorbing ions are designated by M^{+3} and M^{+2} respectively, then M^{+3} will be photoreduced analogous to eqn. [2],

$$\tfrac{1}{2}\,H_2O + M^{+3}\,(aq) \xrightarrow{h\nu} M^{+2}\,(aq) + H^{+} + \tfrac{1}{4}\,O_2, \qquad [5]$$

and the reduction product M^{+2} will be photooxidized analogous to eqn. [3]

$$H^{+} + M^{+2}\,(aq) \xrightarrow{h\nu} M^{+3}\,(aq) + \tfrac{1}{2}\,H_2. \qquad [6]$$

The sum of eqns. [5] and [6] amounts to a decomposition of water

$$\tfrac{1}{2}\,H_2O \rightarrow \tfrac{1}{2}\,H_2 + \tfrac{1}{4}\,O_2. \qquad [7]$$

This particular combination has been realized experimentally only once,[29] and some of the other combinations apparent from Tables I and II should be tried.

Since the definition of electron transfer spectra is empirical, it is important to gather some chemical proof (as opposed to spectroscopic observations) for the existence of these spectra. The question then is whether the chemical products which should result from the photochemical electron transfer have actually been isolated and identified. This has been done in only a few cases of the reductive spectra. The difficulty in the case of reductive spectra lies not only in the well-known capriciousness of the equilibrium

$$2\,OH \rightleftharpoons H_2O_2 \rightleftharpoons H_2O + \tfrac{1}{2}\,O_2, \qquad [8]$$

but also in the hydrolysis of many ions of the transition

* This research was supported by the United States Air Force under contract No. AF 18(603)-7 monitored by the Air Force Office of Scientific Research of the Air Force Research and Development Command.

VOL. 4 1960

TABLE I—Reductive Spectra

Species	$\lambda_{max.}$ mμ	Log $\epsilon_{max.}$	References	ΔF^0_{form} Kcal/mole	K_{inst}	Electron Affinity Volts	Ionization Potential Volts
ZnI_4^{-2}	238.5		1	—		3.28	17.960
$CdCl_4^{-2}$	187.5		1	—		3.78	16.9052
$CdBr_4^{-2}$	215.5		1	—		3.56	16.9052
CdI_4^{-2}	257		1	—	$\sim 5 \times 10^{-7}$	3.28	16.9052
$SnCl_4^{-2}$	218.5	4.5	1	—		3.78	14.63
$SnBr_4^{-2}$	245	4.5	1	—		3.56	14.63
SnI_4^{-2}	290	4.5	1	—		3.28	14.63
Hg^{+2} (aq)	180		1	+39.38			18.752
$HgCl_4^{-2}$	228.5		1	−107.7	8.3×10^{-16}	3.78	18.752
$HgBr_4^{-2}$	250		1	−88.0	2.3×10^{-22}	3.56	18.752
HgI_4^{-2}	323		1	−51.15	5.3×10^{-31}	3.28	18.752
Cu^{+2} (aq)	200		1	+15.53			20.287
$CuCl_4^{-2}$	250		1	—		3.78	20.287
$CuBr_4^{-2}$	281		1	—		3.56	20.287
Pb^{+2} (aq)	208.5	4.0	1	−5.81			15.03
$PbCl_4^{-2}$	272		1	—		3.78	15.03
$PbBr_4^{-2}$	304	4.3	1	—		3.56	15.03
	225	4.9					
PbI_4^{-2}	367.3		1	−63.02		3.28	15.03
$PbCl^+$	226	4.07	1	—	0.0775	3.78	15.03
$PbBr^+$	235.8	4.29	1	—	0.071	3.56	15.03
PbI^+	264.5	4.33	1	—	0.0345	3.28	15.03
Fe^{+3} (aq)	~230	3.7	1, 5	−2.53			43.43
$FeCl^{+2}$	~320	3.6	1	−35.9	0.03	3.78	43.43
$FeBr^{+2}$	~380	3.9	1	−27.9	0.25	3.56	43.43
$FeCNS^{+2}$	~460	3.8	1, 6	—	1.04×10^{-3}		43.43
$Fe(CN)_5NO^{-2}$	260	3.9	7				43.43
Ce^{+4}	~320	3.7	1, 8, 9	$\Delta H^0_{form} = -134.4$			16.6
UCl_4	300 (absorption edge)		10	crystal −230.0		3.78	
$Co(C_2O_4)_3^{-3}$	245		11				33.49
$Co(C_2O_4)_3^{-3}$	243	4.21	12				33.49
$Co(NH_3)_5N_3^{+2}$	302	3.94	13				33.49
$Co(NH_3)_5I^{+2}$	383	3.43	14			3.28	33.49
	286	4.22					
$Co(NH_3)_5Br^{+2}$	314.5	2.91	14	$\Delta H^0_{form} = -152.7$		3.56	33.49
	253	4.27					
$Co(NH_3)_5Cl^{+2}$	274	2.65	14		10^{-33}	3.78	33.49
	227	4.31					
$Cr(NH_3)_5I^{+2}$	290.5	3.60	14			3.28	29.8
$Co(NH_3)_5NO_2^{+2}$	325	3.22	15		$\sim 10^{-34}$		33.49
	238.5	4.14					
$Co(NH_3)_4(NO_2)_2^+$ cis	324	3.62	15		$\sim 10^{-34}$		33.49
	234	4.28					
$Co(NH_3)_4(NO_2)_2^+$ trans	347	3.68	15				33.49
	252.5	4.26					
$Co(NH_3)_3(NO_2)_3$	242	3.84	15				33.49
	252	4.26					
$Co(NO_2)_6^{-3}$	358	3.85	12				33.49
	267	4.09					
$Co(NH_3)_4(N_3)_2^+$ cis	303	4.01	16				33.49
$Co(NH_3)_4(N_3)_2^+$ trans	337	4.14	16				33.49
$Co(NH_3)_3(N_3)_3$	335	4.05	16				
$Co(NH_3)_4Cl_2^+$ trans	303.5	2.86	17	$\Delta H^0_{form} = -173.4$		3.78	33.49
	253.5	4.39					
$Co(En)_2Cl_2^+$ cis	312	2.77	17			3.78	33.49
	240	4.28	18				
$Co(En)_2Cl_2^+$ trans	307.5	3.12	17			3.78	33.49
	248.5	4.43					
$Co(En)_2Br_2^+$ trans	356	3.35	17			3.56	33.49
	289	4.34					
$Co(NH_3)_5NCS^{+2}$	305	3.18	19				33.49
$Co(NH_3)_5ONO^{+2}$	362	2.44	19				33.49
$Cr(NH_3)_5ONO^{+2}$	356	1.90	19				29.8
$Cr(NH_3)_5SCN^{+2}$	300	3.76	19				29.8
$Cr(NH_3)_5N_3^{+2}$	263	3.70	19				29.8
$Fe(C_2O_4)_3^{-3}$			20		$\sim 10^{-23}$		27.32
$CoEn_2(NO_2)_2^{+(1)}_{(6)}$ trans	339	3.44	21				33.49
	249	4.37					
$Co(NH_3)_4ClNO_2$ trans	338	3.13	21				33.49
	244	4.07					
$CoEn_2ClNO_2$ trans	335	3.37	21				33.49
	242	4.35					

TABLE II—Oxidative spectra

Species	λ_{max} mμ	Log ϵ_{max}	E° Kcal/mole	Reference
OH^-	186	3.6		22
Cl^-	184	3.7	56	23
	179			
Br^-	201	3.9		
	188	4.08	44	23
I^-	194			
	(232)	4.11	29	23
	λ_t			
Co^{+2}	220	—	42	24
Ni^{+2}	220	—	—	24
Mn^{+2}	225	—	35	24
Fe^{+2}	285	—	18	24
V^{+2}	~350	—	−5	24
Cr^{+2}	~380	—	−9	24
Eu^{+2}	~366	—	−10	25
ClO_3^-	225	—	—	26
BrO_3^-	270	—	—	26
IO_3^-	290	—	—	26

TABLE III

Species	λ_{max} mμ	$\Delta F°_{form}$, kcal/mole	Electron Affinity volts	Ionization Potential volts
$HgCl_4^{-2}$	228.5	−107.7	3.78	18.752
$HgBr_4^{-2}$	250	−88.0	3.56	18.752
HgI_4^{-2}	323	−51.15	3.28	18.752

elements. When more than one valence state exists, the hydrolysis is usually more pronounced in the higher-valent ion. The evolution of oxygen has been confirmed in the photochemical reduction of ferric ions. The course of the reaction

$$Ce^{+4}\cdot H_2O \xrightarrow{h\nu} Ce^{+3} + H^+ + OH \rightarrow \text{products} \qquad [9]$$

has been elucidated in several publications.[8, 9, 28, 29, 30]

In those complex ions in which the photoexcitation transfers the electron to a ligand other than water or a hydroxyl ion, chemical proof of the photochemical electron transfer has been obtained. For example, $Co(NH_3)_5N_3^{+2}$ undergoes the primary reaction

$$Co(NH_3)_5N_3^{+2} \xrightarrow{h\nu} Co^{++} + N_3 + 5NH_3 \qquad [10]$$

with the ultimate formation of nitrogen in amounts corresponding to the azide ion originally present.[13]

Chemical proof has also been obtained of the reduction of $Fe(C_2O_4)_3^{-3}$ to $Fe(C_2O_4)_3^{-2}$ in sunlight[20] and of UCl_4 to UCl_3 upon irradiation.[10]

Chemical proof is easier to obtain for the oxidative electron transfer spectra. For instance, evolution of hydrogen occurs in the photooxidation of halide ions according to eq. [4]. Furthermore, the quantum yield of this reaction increases with acid concentration, as would be expected for the production of hydrogen.[31] As a matter of fact, enough studies have been done on hydrogen evolution from halide photooxidation that hydrogen-isotope separation has been observed.[32] Hydrogen formation has also been observed in the photooxidation of transition-element ions (eqn. 3) in acid solutions. Furthermore, hydrogen atom formation has been demonstrated in these latter reactions by polymerization initiation techniques.[24]

The energetics involved in electron transfer spectra have also been examined. Since these absorption peaks are primarily a characteristic of the particular complex ion, it is no surprise to find their wave length varying with the standard free energy of formation for a homologous series of complexes. Thus, the data of Table III show that for three polyhalide complexes of mercuric ion, the electron transfer peak moves toward the visible (less energy is required to excite electron transfer spectrum) as the complex ion becomes less stable, i.e., has a less negative standard free energy of formation.

It is quite apparent that the electron transfer spectra are a function of the ionization potential of the central ion and of the electron affinity of the ligand. This is particularly evident for a series such as that listed in Table III, where the ionization potential is constant: the electron transfer peak moves toward the visible as the electron affinity decreases (less energy is required to move the electron). However, the situation is much less clear when one considers electron transfer from water to a metal ion according to eqn. [2]. A number of such cases are listed in Table IV.

The energetics are much clearer for the oxidative spectra. The wave lengths of the halide electron transfer peaks have been adequately predicted by the ex-

TABLE IV

Species	λ_{max} mμ	$\Delta F°_{form}$, kcal/mole	Ionization Potential volts
Hg^{+2} (aq)	180	+39.38	18.752
Cu^{+2} (aq)	200	+15.53	20.287
Pb^{+2} (aq)	208.5	−5.81	15.03
Fe^{+3} (aq)	230	−2.53	43.43
Ce^{+4} (aq)	320	−134.4 ($\Delta H°_{form}$)	16.6

TABLE V

Species	λ_{edge} mμ	$\frac{hc}{\lambda_{edge}}$ kcal/mole	E° kcal/mole	Ionization Potential volts	$E^\ddagger$ kcal/mole
Co^{+2}	220	129	42	33.49	39
Ni^{+2}	220	129	—	—	—
Mn^{+2}	225	125	35	(32)	42
Fe^{+2}	285	100	18	43.43	34
V^{+2}	350	81	−5	26.4	38
Cr^{+2}	380	75	−9	29.8	36

$$E^\ddagger = \frac{hc}{\lambda_{edge}} - E^\circ_{M^{++}\text{-}M^{+++}} - E^\circ_{H-H^+}.$$

VOL. 4 1960

pression

$$h\nu = A + H_{ion} - 0.9 \text{ ev}, \qquad [11]$$

where A is the halogen electron affinity and H_{ion} is the heat of solution of the halide ion.[31] The oxidative electron transfer spectra of transition element ions (eqn. 3) have not been examined in this manner. The absorption edges of some of these electron transfer spectra are shown in Table V, together with the oxidation potential of the corresponding half-cell and the ionization potentials. The trend of the absorption edges corresponds only very roughly to the trend of the ionization potentials, but corresponds much better to the trend of the oxidation potentials.

This implies, as would be expected, that with increasing stability of the oxidized metal ion, less energy (longer wave lengths) is required to transfer an electron from the metal central ion to the ligand water. Since hydrogen atoms are produced as intermediates in this reaction, the oxidation potential for hydrogen atom formation (48.57 kcal/mole) and the oxidation potential of the metal couple have been subtracted from energy corresponding to the electron transfer spectrum. This difference, shown in the last column of Table V, is surprisingly constant. This constancy suggests that further analysis of this difference will reveal some factors common to each of these reactions.

REFERENCES

1. Rabinowitch, E. *Rev. Mod. Phys.* **14,** 112–31 (1942)
2. Orgel, L. E. *Quart. Revs.* (London) **8,** 422–50 (1954)
3. Amphlett, C. B. *Quart. Revs.* (London) **8,** 219–49 (1954)
4. Benesi, H. A. and J. H. Hildebrand. *J. Am. Chem. Soc.* **70,** 2832–3 (1948)
5. Saldick, J. and A. O. Allen. *J. Am. Chem. Soc.* **77,** 1388–90 (1955)
6. Betts, R. H. and F. S. Dainton. *J. Am. Chem. Soc.* **75,** 5721–7 (1953)
7. Samuel, R. *Physik* **70,** 43–73 (1931)
8. Sworski, T. J. *J. Am. Chem. Soc.* **77,** 1074–5 (1955)
9. Weiss, J. and D. Porret. *Nature* **139,** 1019–20 (1937)
10. Freed, S. and K. M. Sancier. *J. Chem. Phys.* **22,** 928–9 (1954)
11. Copestake, T. B. and N. Uri. *Proc. Roy. Soc.* (London) **A228,** 252–63 (1955)
12. Kiss, A. and D. v. Czegledy. *Z. anorg. allgem. Chem.* **235,** 407–26 (1938)
13. Linhard, M. and H. Flygare. *Z. anorg. Chem.* **262,** 328–43 (1950)
14. Linhard, M. and M. Weigel. *Z. anorg. Chem.* **266,** 49–72 (1951)
15. Linhard, M. and M. Weigel. *Z. anorg. Chem.* **267,** 113–20 (1952)
16. Linhard, M. and G. Stirn. *Z. anorg. allgem. Chem.* **268,** 105–27 (1952)
17. Linhard, M. and M. Weigel. *Z. anorg. allgem. Chem.* **271,** 101–14 (1952)
18. Basolo, F. *J. Am. Chem. Soc.* **72,** 4393–7 (1950)
19. Linhard, M., H. Siebert and M. Weigel. *Z. anorg. allgem. Chem.* **278,** 287–99 (1955)
20. Sastri, M. N. and Ch. Kalidas. *Z. anal. Chem.* **149,** 181–4 (1956)
21. Kuroya, H. and R. Tutida. *Bull. Chem. Soc. Japan* **15,** 427–39 (1940)
22. Ley, H. and B. Arends. *Z. physik. Chem.* **B 6,** 240–6 (1930)
23. Scheibe, G. *Z. physik. Chem.* **B 5,** 355–64 (1929)
24. Dainton, F. S. and D. G. L. James. *J. chim. phys.* **48,** Nos. 9, 10, C 17–22 (1951)
25. Douglas, D. L. and D. M. Yost. *J. Chem. Phys.* **17,** 1345–6 (1949)
26. Farkas, L., and F. S. Klein. *J. Chem. Phys.* **16,** 886–93 (1948)
27. Marcus, R. J. *Science* **123,** 399–405 (1956)
28. Heidt, L. J. and M. E. Smith. *J. Am. Chem. Soc.* **70,** 2476–81 (1948)
29. Heidt, L. J. and A. F. McMillan. *Science* **117,** 75–6 (1953)
30. Marcus, R. J. and H. C. Wohlers. *Ind. Eng. Chem.* **51,** 1335 (1959)
31. Platzman, R. and J. Franck, in *L. Farkas Memorial Volume*, A. Farkas and E. P. Wigner, Eds. Research Council of Israel, Jerusalem, 1952
32. Farkas, A. and L. Farkas. *Trans. Faraday Soc.* **34,** 1113–20 (1938)

Selectively Emissive Materials for Solar Heat Absorbers

R. B. Gillette

Aero-Space Division, Boeing Airplane Company, Seattle, Washington

Space-vehicle power requirements have created a need for developing devices that efficiently convert solar energy to electricity. For a high conversion efficiency in thermal systems, an absorbing surface must have high solar absorptivity and low infrared emissivity. Consequently, research was aimed at obtaining selectively emissive materials for solar heat absorbers. A theoretical analysis was made of absorber-surface efficiencies and selective absorber materials were prepared and tested. The theoretical analysis showed that selective absorbers do have an efficiency advantage over black-body surfaces at temperatures up to 3000 F. Two good selective coatings were developed—a cobalt-oxide deposit and a chrome-nickel-vanadium deposit. The coatings were applied to both polished copper and nickel. The cobalt-oxide surfaces produced an absorptivity of 0.93 and an infrared emissivity of 0.24. The chrome-nickel-vanadium surface had an absorptivity of 0.94 and an infrared emissivity of 0.40.

INTRODUCTION

Space-vehicle power requirements have created a need for developing devices that efficiently convert solar energy to electricity. Various thermal conversion devices, such as thermoelectric, thermionic, and mercury turbine heat engines, are being explored. These processes require a high temperature to give a high conversion efficiency because of Carnot cycle considerations. The present operating temperatures for these devices range from 1000 to 3000 F.

A typical solar conversion system is made up of three components:

a) A concentrator, which focuses solar radiation from a large intercepting area into a small area (the focus);

b) An absorber, which converts the radiation in the focus into useful heat;

c) A conversion device or heat engine, which produces work or electricity from the absorbed heat.

The replacement of conventional cavity-type (black) absorber surfaces with newly developed, selectively emissive coatings has significantly decreased the absorber radiation loss with a resultant improvement in overall solar conversion efficiencies.

Considerable research has been done by Daniels, Tabor, Hottel, et al., in developing selectively emissive coatings for terrestrial applications.[1, 2] Their research produced coatings with absorptivities as high as 0.92 and emissivities as low as 0.11. Promising coatings that were used successfully are thin films of copper oxide, cobalt oxide, and other black oxides placed on highly polished, low-emissivity metal. The objective of this research has been to develop a coating with high solar absorptivity (α) and a low thermal emissivity (ϵ) that will withstand the oxidizing environment of the atmosphere.

The present research in selective emissivity has been directed toward preparing a coating that will not sublime at a high temperature (greater than 1000 F) in the high-vacuum environment of space. One-quarter wave-length interference filters were considered but rejected because of their rapid sublimation at high temperatures. The approach taken involves the application of a selectively transparent film (about one wave length thick) onto a highly polished (low-emissivity) metal base.

THEORETICAL ANALYSIS

The performance of an ideal selective absorber was compared with a black-body absorber at temperatures beyond those reported in the references. To analyze absorber performance, the radiation emission spectrum of a black body was compared with the emission spectrum of the sun as shown in Fig. 1. It should be noted in Fig. 1 that the incident solar energy has been concentrated 640 times to equal the radiation heat flux from a black body at 3140 F. Thus, if the absorbing surface is a black body (i.e., spectral emissivity is unity at all wave lengths), all impinging solar energy is absorbed and all of the black-body spectrum is emitted. No heat is retained to produce useful work.

Theoretically, an ideal selective absorber at 3140 F absorbing solar radiation would absorb all radiation of wave lengths shorter than 1.2 microns and would reflect all radiation longer than 1.2 microns. By definition the selective absorber also would radiate the

VOL. 4 1960

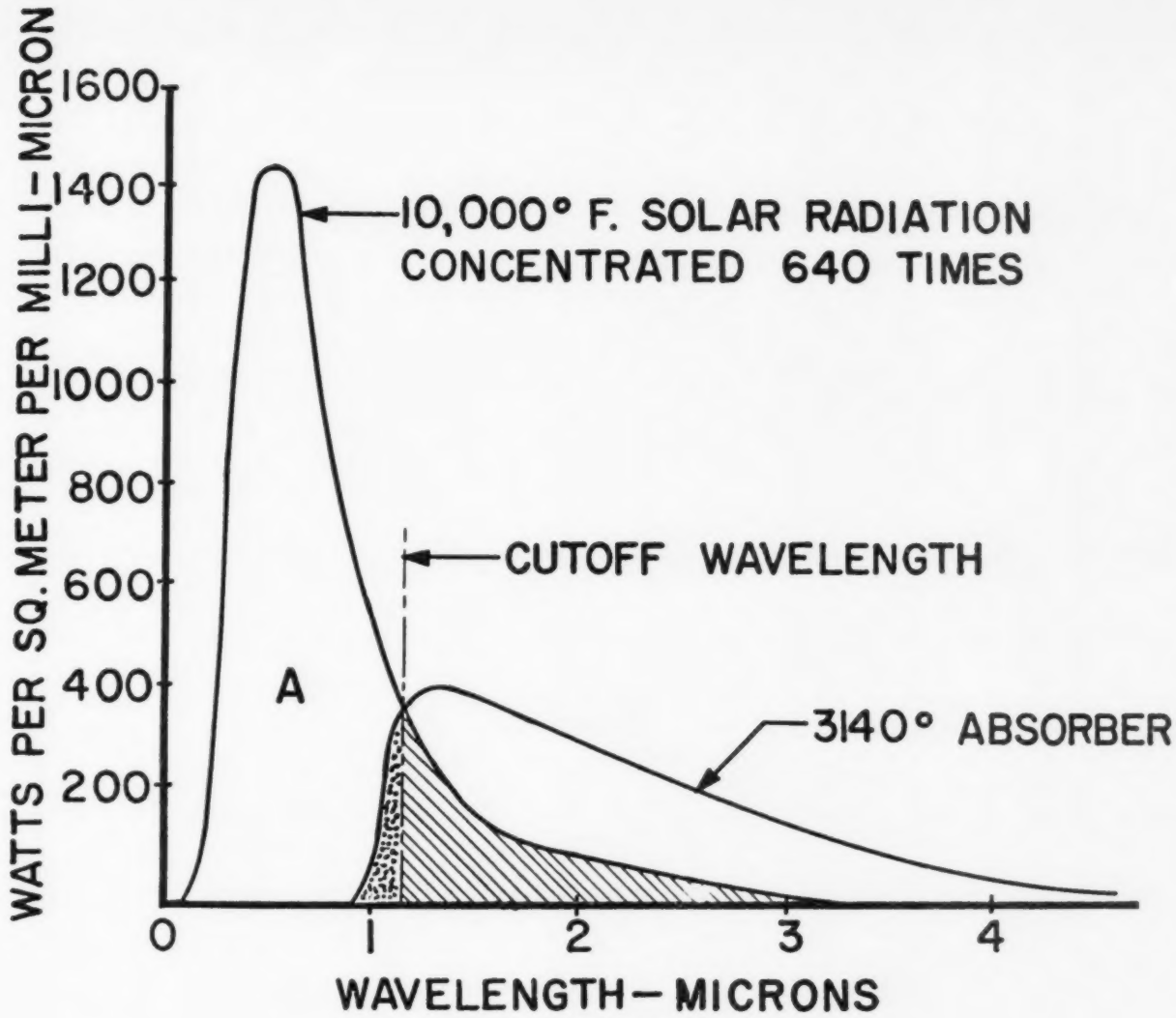

FIG. 1—Radiation spectra.

portion of the black-body spectrum to the left of the cutoff because its spectral emissivity is unity in that region. Thus, the total loss from the ideal selective surface is represented by the crosshatched area, and the heat retained is represented by the area A.

A measurement of the quality of an absorbing surface is absorption efficiency.

$$\text{Absorption efficiency} = \frac{\text{Net heat absorbed}}{\text{Gross available heat}}$$

Using this definition and referring to the conditions of Fig. 1, the efficiency is zero for the 3140 F black-body absorber and 66 per cent for the ideal selective absorber. Absorption efficiency can be calculated using various concentration ratios for both a black body and a selective absorber at 3140 F, where concentration ratio is defined as

$$\text{Concentration ratio} = \frac{\text{Heat flux incident on absorber}}{\text{Solar heat flux incident on mirror}}$$

The results of a typical calculation are shown in Fig. 2. The efficiency of the black-body absorber is zero at a concentration ratio of 640 because the absorbed solar radiation for that condition exactly equals the reradiation and, therefore, no net heat is absorbed. Increasing the concentration ratio while extracting useful heat to maintain a constant temperature causes a rapid increase in efficiency until it levels off at 60 to 70 per cent. Substituting an ideal selective absorber at a concentration ratio of 640 gives an absorption efficiency of 66 per cent. Increasing the concentration ratio while using the selective absorber gives only a slight increase in efficiency. At higher concentration ratios, the two curves become parallel and the use of a selective absorber has only a small advantage over the black body.

A quantitative analysis of the radiation spectrums shows that the optimum absorption cutoff wave length is at the intersection of the solar spectrum and the

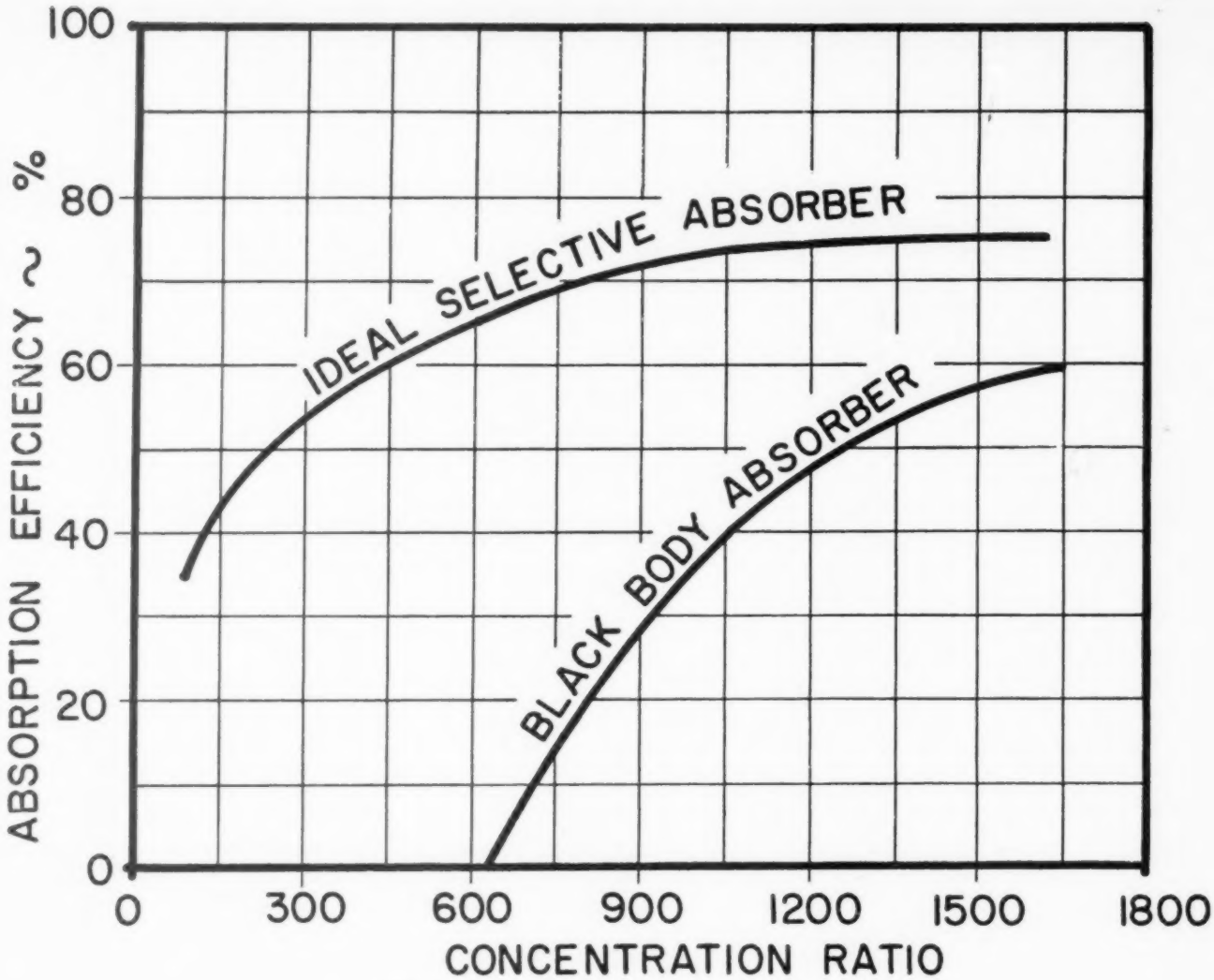

FIG. 2—Absorption efficiency for 3140 F surface.

emission spectrum. As the concentration of solar energy is changed while maintaining a constant absorber temperature, the optimum cutoff wave length changes because the intersection occurs at a different wave length. Fig. 3 shows the effects of concentration ratio on the optimum cutoff wave length using various absorber temperatures. It can be observed from this illustration that, as absorber temperature increases, the optimum cutoff wave length shifts to shorter wave lengths and varies less with concentration ratio. It is concluded that the optimum cutoff wave length must be achieved more precisely at the higher absorber temperatures.

EXPERIMENTAL WORK

The experimental program involved testing selectively coated samples by two methods: a thermal emissometer and a solar emissometer. The thermal emissometer used can determine total emissivities at temperatures varying from 500 to 1800 F by measuring normal radiation from a test specimen and comparing this radiation to that emitted by a black-body standard. The accuracy of measurements by this device is within 10 per cent above 1000 F and 15 per cent at 600 F and lower. The solar emissometer can measure both solar absorptivity and thermal emissivity from 300 to 800 F in a vacuum of 5 to 10 microns of mercury. This device exposes the test specimen to two different, concentrated solar heat fluxes, which are provided by a 9-inch and 12-inch diameter Fresnel lens opening, respectively. The absorptivity and emissivity can then be calculated from two simultaneous heat-balance equations. By substituting readings taken from both measurements into each equation, the heat flow to and from the sample plus the rate of change in heat content of the sample can be described. The equations *are* written for the

VOL.
4
1960

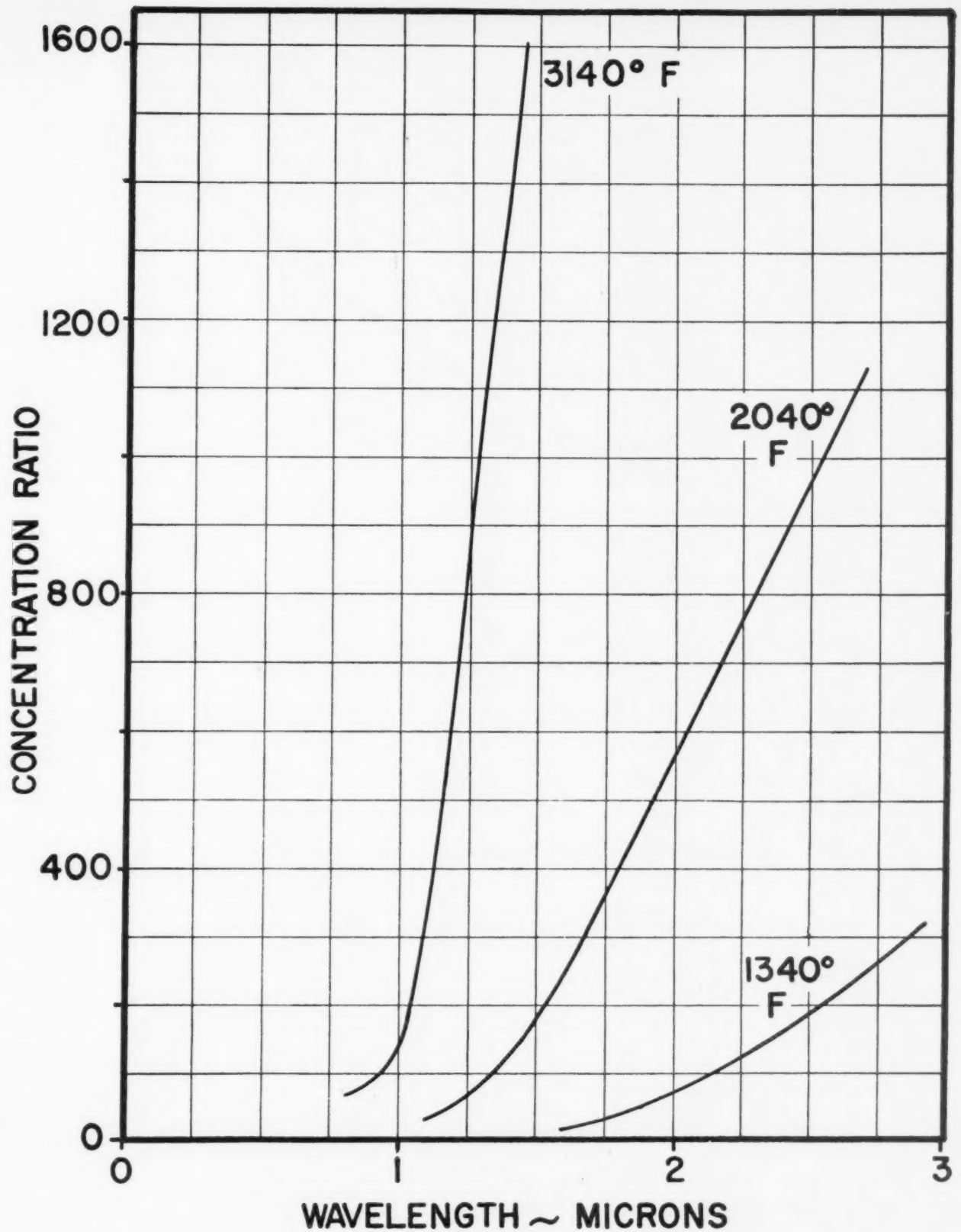

FIG. 3—Optimum cutoff wave length.

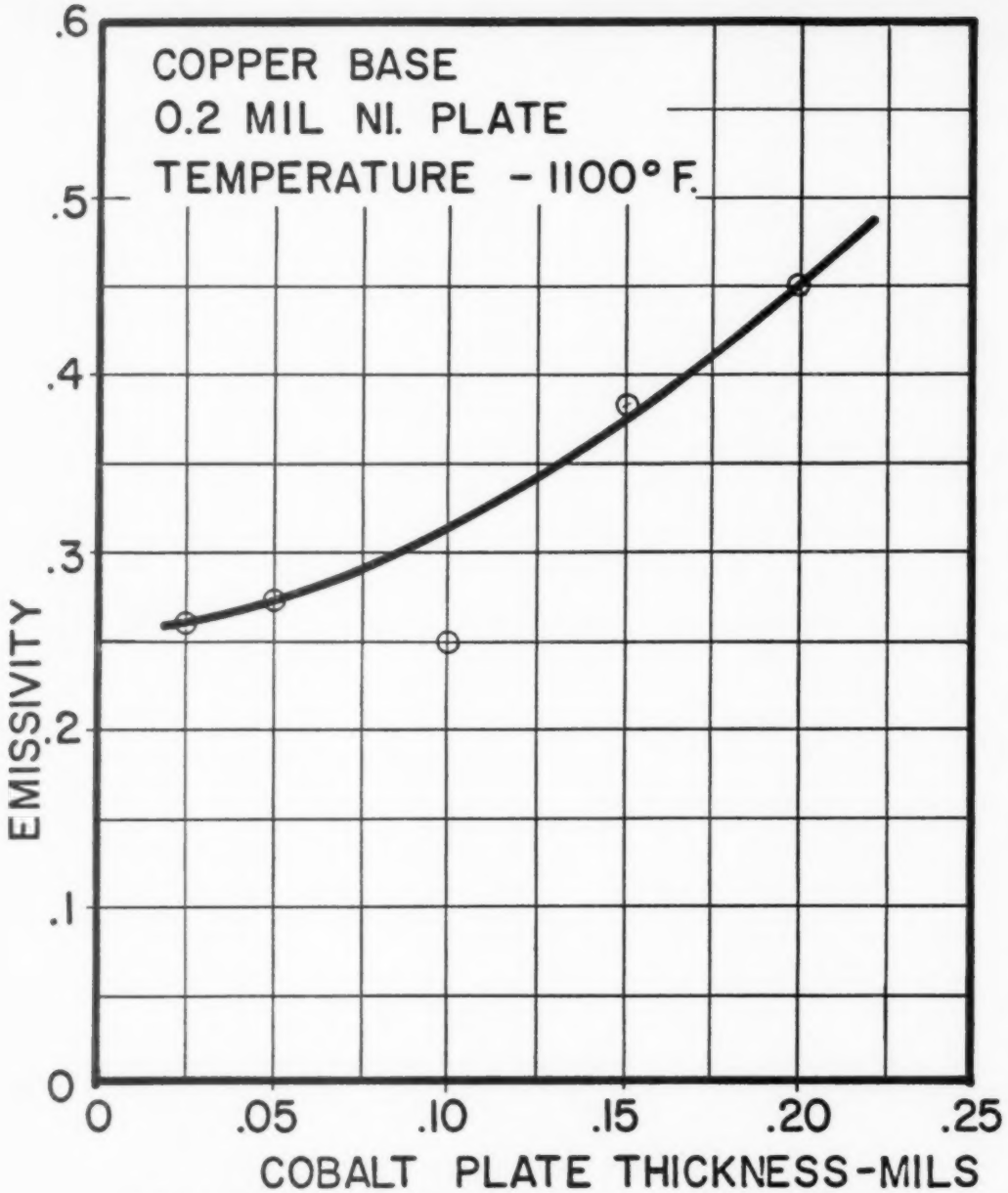

FIG. 4—Effect of cobalt thickness on emissivity of cobalt oxide surface.

same temperature but different incident heat fluxes. Accuracy of α and ϵ computed in this manner has been shown to be ± 15 per cent.

Many specimens were prepared and tested; however, data from only the most promising coatings will be described here. The basic specimen material used was copper; its surface was polished and buffed until highly reflective. The specimens tested in the solar emissometer had the oxide coating placed directly on the polished copper. For the thermal emissometer tests, it was necessary to apply a 0.2-mil nickel coating to the copper before application of the oxide. The nickel was needed to prevent oxidation of the copper because the thermal emissometer could only maintain a vacuum of 110 to 120 microns of mercury. It was believed initially that a vacuum of 1 to 10 microns in the solar-emissometer chamber would be enough to prevent oxidation of the copper. However, it was found that the samples did oxidize under these conditions and increased emissivity resulted.

The two most promising coatings developed were cobalt oxide and a chrome-nickel-vanadium alloy plate. The cobalt oxide was obtained by first plating the cop-

VOL.
4
1960

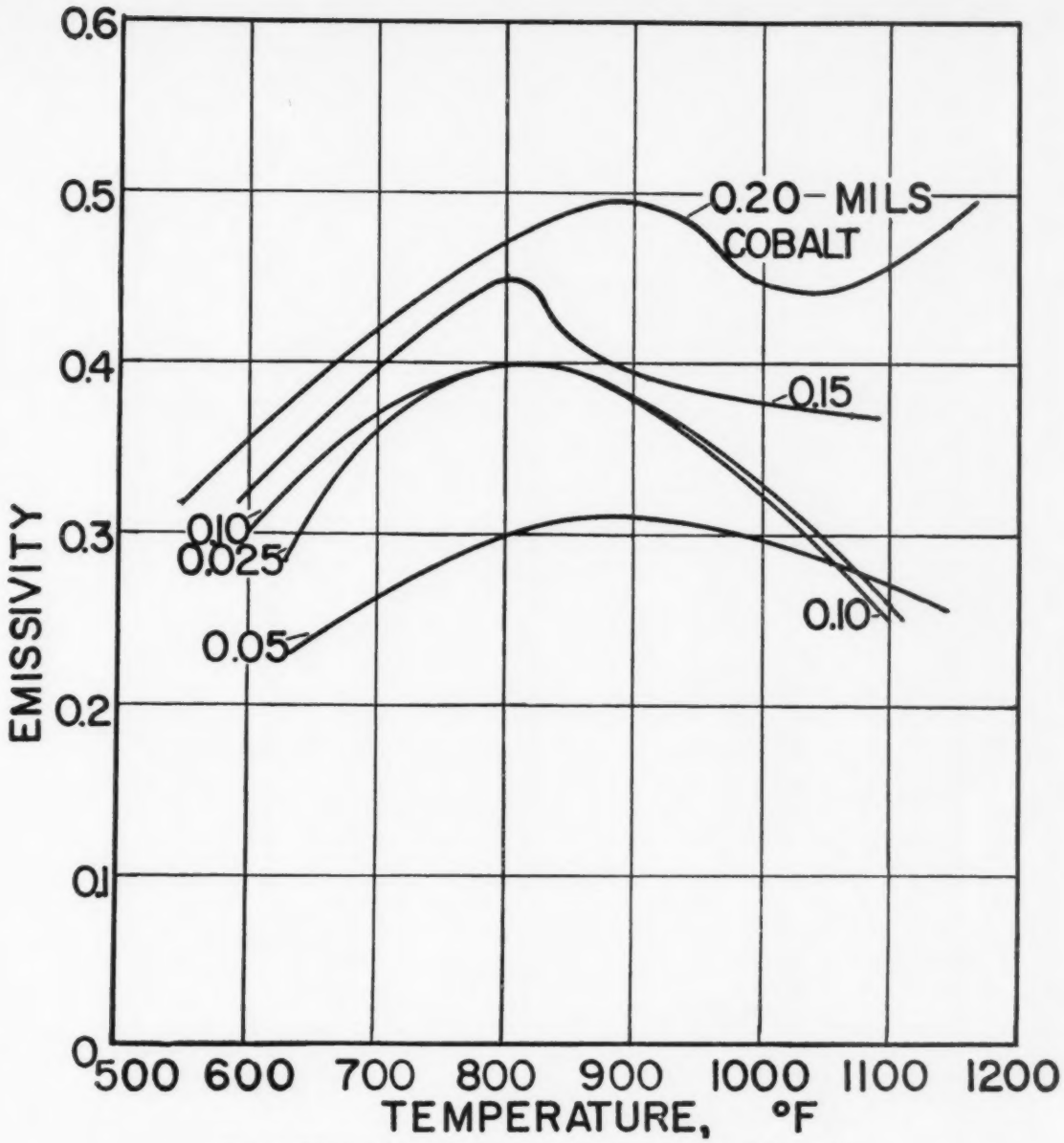

FIG. 5—Effect of temperature on emissivity of cobalt oxide surface.

per or nickel with pure cobalt and then anodizing the surface.

The cobalt plating was done with a bath containing 500 grams per liter of $CoSO_4 \cdot 7H_2O$, 15 grams per liter NaCl, 40 grams per liter of H_3BO_3, and 0.05 grams per liter of Duponal powder. The Duponal is an additive that prevents pitting of the surface. The plating was done at 70 amps per square foot in a 130 F solution for times varying from 45 seconds to 6 minutes. A sheet of 317 stainless steel was the anode. The anodizing solution contained 40 per cent by weight of potassium hydroxide in water. The conditions of anodization were 10 amps per square foot in a 70 F solution for 4 minutes.

In this cobalt-oxide surface preparation, it was observed that a cobalt plate thickness of less than 0.02 mil (0.5 micron) was the thinnest practical coating. Coatings thinner than this were transparent to solar radiation, which peaks around 0.6 micron, and exhibited sharply decreased absorptivity.

The Cr-Ni-Va alloy coating was prepared by plating, in a bath containing 250 grams per liter of CrO_3, 36 grams per liter of $NiCl_2 \cdot 7H_2O$, 14 grams per liter of NH_4VO_3, and 10 grams per liter of CH_3COOH. The conditions of plating were 800 amps per square foot in an 85 F solution for 1 minute using Pb-7% Sn anode. The actual absorptive coating was a powdery, brown

oxide that was deposited during the Cr-Ni-Va plating. It was observed that the process control of this surface was not as good as the preparation of the cobalt coating (i.e., the brown deposit was quite sensitive to solution temperature, current density and other plating conditions). Furthermore, the absorptive coating could be rubbed off readily by hand.

The emissivity tests made on the specimens with the thermal emissometer produced the following results: The emissivity of the cobalt-oxide coatings was found to vary from 0.24 to 0.45 for thicknesses of cobalt varying from 0.025 to 0.20 mil (Fig. 4). The optimum thickness appears to be about 0.05 mil, which produces an emissivity of 0.28 at 1100 F. The emissivity that corr-e sponds to a thickness of 0.1 mil does not fall on the curve because much of the coating flaked off, exposing the low-emissivity nickel. This sample would have a low solar absorptivity.

An interesting effect was observed when the temperature of the cobalt specimens was varied (Fig. 5). The emissivity increased with temperature up to about 800 F and then decreased up to the maximum observed temperature of 1100 F. In several cases the emissivity at 1100 F actually was lower than that at 650 F. For

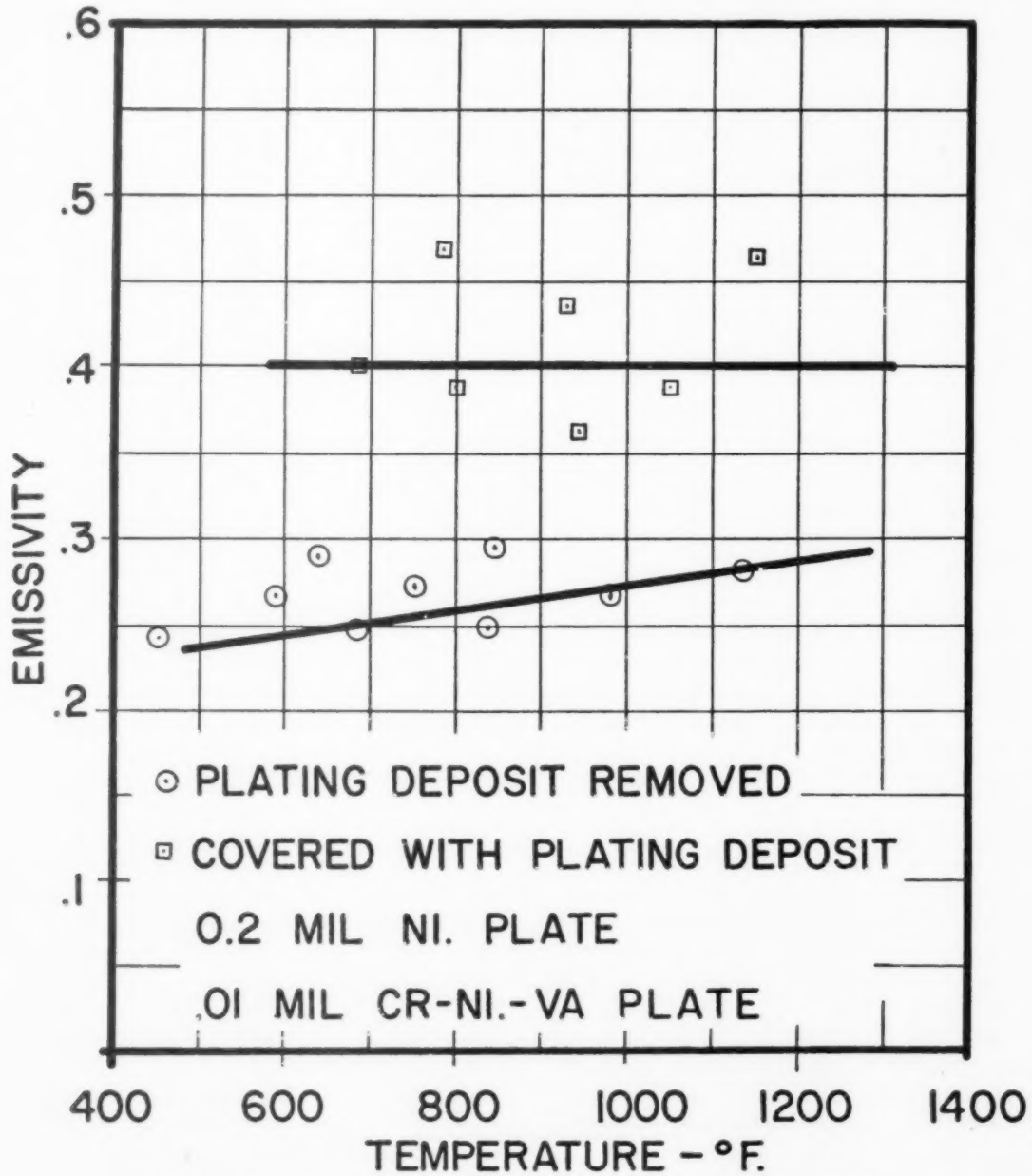

FIG. 6—Effect of temperature on emissivity of chrome-nickel-vanadium surface.

VOL. 4 1960

three specimens, the emissivity reached a minimum at 1000 to 1100 F and then started to increase with temperature similar to the increase experienced in the range less than 800 F.

This unusual emissivity variation could be explained in several ways. It is possible that the oxide film sublimed and thus became thinner. Past investigations have not found this sublimation at high temperature in air to be significant. Inspection clearly indicated that sublimation had occurred on one of the samples. A second explanation of the unusual emissivity variation could be that certain metallic oxides exhibit a decrease in emissivity with increasing temperature throughout this temperature range. If this effect is true, selective cobalt coatings appear even better than expected at temperatures above 800 F because it was formerly assumed that their emissivity would increase steadily with temperature. Additional tests are being made to explore this effect. A third explanation may be that the molecular structure of cobalt oxide may have altered at about 800 F. This could explain the sharp change in emissivity characteristics. This possibility was not explored.

Several observations were made of the mechanical stability of the cobalt-oxide coatings. It should be noted that the anodization current density and time were fixed for all the coatings, but the thickness of the cobalt plate was varied. Thus, the thinnest cobalt coatings were oxidized through to the base nickel, and the thickest were only partly oxidized. Referring to Fig. 5, the 0.05 and 0.20 mil thickness coatings were stable throughout the entire temperature range, whereas the remainder of the specimens spalled or flaked off, exposing some of the nickel. It was also observed that the coatings thinner than 0.05 mil had oxidized completely through in the anodization process. This resulted in a low-durability coating that could be scraped off easily with a fingernail. The coatings, 0.05 mil and thicker, were adherent to the base metal and could not be scraped off. In general, the optimum coating from the emissivity standpoint appears to be 0.05 mil of cobalt.

The results of the thermal emissometer tests of the Cr-Ni-Va coatings are shown in Fig. 6, which plots emissivity versus temperature for four specimens, each having a deposit of Cr-Ni-Va about 0.01 mil thick. The thickness of the brown oxide that deposited on the Cr-Ni-Va alloy was unknown. The curve of highest emissivity represents the two samples having the oxide coating left on, and the curve of lowest emissivity represents the two samples with the oxide removed. It can be seen that the oxide-coated specimens have a constant emissivity of 0.4 and the uncoated samples have an emissivity of about 0.27. It should be noted that, although removing the coating lowers the emissivity, the solar absorptivity will also be decreased substantially.

The thermal stability of the Cr-Ni-Va coating was good in that no spalling occurred with these specimens. It was observed that the oxide film changes from a light brown to a dark green during heating. The stability of this coating is better than the cobalt-oxide coatings; however, it is easily rubbed off. No serious oxidation of either Cr-Ni-Va or cobalt-oxide coatings occurred in the 100 microns of mercury vacuum environment of the thermal emissometer.

The measurements in the solar emissometer were made on the same type of coatings used in the thermal emissometer, except that the samples were prepared by depositing the selective coating directly onto the polished copper. The actual emissivities and absorptivities were calculated from data taken between 400 and 600 F.

The solar absorptivity of the cobalt-oxide sample was found to be about 0.93 and the emissivity about 0.24, as measured in the solar emissometer. These values represent a cobalt thickness of 0.20 mil. Visual observations indicate that nearly the same absorptivity exists for the coating of 0.05-mil thickness; however, a surface with a coating thinner than 0.02 becomes reflective to light and, thus, has a lower absorptivity.

It was found that the cobalt-oxide coated specimen oxidized considerably even when using a vacuum of 5 to 10 microns of mercury and initially purging with argon. No spalling occurred, but the thickness of the cobalt oxide and copper oxide increased and, thus, the emissivity increased.

The solar absorptivity of the Cr-Ni-Va was found to be about 0.94, as measured in the solar emissometer. The coating exhibited excellent stability in the vacuum of 5 to 10 microns. No spalling or oxidation occurred during a 10-hour heating test at 800 to 1000 F. The brown oxide turned dark green as did the specimens tested in the thermal emissometer.

Further studies are exploring the stability of both cobalt oxide and Cr-Ni-Va coatings in vacuum at high temperatures for extended times. The correlation of spalling with cobalt thickness and anodization parameters also should be examined. An explanation for the decrease in emissivity with temperature, experienced with the cobalt coatings, is also an area of interest.

CONCLUSIONS

The following conclusions were made:

1. Selective coatings have a theoretical efficiency advantage over black-body absorbers even at temperatures in excess of 3000 F;

2. Elevated operating temperatures require thinner and more precisely controlled coatings;

3. It is feasible to prepare selective coatings that will withstand a temperature of 1150 F in vacuum; the best

coating considering vacuum stability is the Cr-Ni-Va surface;

4. Present data are insufficient to determine the expected operating life of these selective coatings in space.

REFERENCES

1. Kokoropoulos, P., Salam, E. and Daniels, F. "Selective Radiation Coatings, Preparation and High Temperature Stability." *Solar Energy*, **3,** December, 1959, pp. 19–23.
2. Tabor, H. "Selective Radiation I, Wavelength Discrimination," *Transactions of the Conference on the Use of Solar Energy—the Scientific Basis*, Tucson, 1955. **2,** Part 2, p. 24.
3. Hottel, H. C., Unger, T. A. "The Properties of a Copper Oxide-Aluminum Selective Black Surface Absorber of Solar Energy, *Solar Energy* **3,** October, 1959, pp 10–15.
4. Oman, H., Street, G. "Experimental Solar Thermionic Converter for Space Use." Submitted for the AIEE Pacific General Meeting, San Diego, California, August 8–12, 1960.

VOL.
4
1960

Randomly Rotating, Spherically Arrayed Silicon Solar Energy Converters

Werner Luft

Chief Design Engineer, International Rectifier Corporation, El Segundo, California

Since spherical arrays of silicon solar cells are contemplated for the photovoltaic conversion of solar energy in certain satellite projects, various aspects of the solar cell matching problem arising from the nonuniform irradiation and temperature in an unoriented randomly spinning converter are discussed, and a sample calculation of power output is given.

INTRODUCTION

Solar energy converters in spherical configuration are contemplated for certain satellite projects. Since the temperature and illumination of such converters is nonuniform at any instant over the entire irradiated area, and since this fact causes difficult matching problems for an unoriented randomly spinning converter, it is timely to discuss some aspects thereon.

First, the influence of irradiation intensity is discussed briefly. At each point over the collector the illumination intensity varies as the cosine of the angle of incidence, and, accordingly, for a spherical collector, cells at different locations on the collector will have a varying output.

Secondly, the effect of cell temperature is described and an equation is presented to determine the cell temperature under certain conditions. It is shown that, under the assumed conditions, the temperature distribution over the surface of a spinning spherical converter follows a definite pattern which depends on the angle which the spin axis makes with the incident radiation.

To a first approximation, the combined effect of illumination intensity and temperature can then be calculated from the presented information for any part of the converter.

The final part of the article describes what effect the series and parallel connection of the cells all over the spherical collector and at different illuminations intensity and temperature have on the total output of the converter. For a randomly rotating converter, the main interest is to determine the minimum output, since this will govern the size of the transmitters and other equipment powered by the solar energy converter. An example is therefore given to show how the minimum output is determined. The maximum output is also of interest, as overcharging of the batteries must be avoided, and ways to calculate it are indicated.

ILLUMINATION INFLUENCE ON OUTPUT CHARACTERISTICS

The amount of incident radiant power affects the power output from a silicon solar cell. In Fig. 1, the relation between illumination intensity, output current, and voltage is illustrated by the curved surface. For any given spectral distribution of the incident radiation, and at constant cell temperature, the output current at zero output voltage, viz. the light current, is directly proportional to the illumination intensity: $I_{sc} = kL$.[1]

At any other constant voltage, the change in the output current varies almost linearly with the change in illumination level, i.e., $\Delta I/\Delta L \simeq$ constant, but the current is not proportional to the illumination level, $(I \neq kL)$. This relationship is seen from the straight, constant voltage lines in Fig. 1.

The output voltage at zero current varies almost as the logarithm of the illumination intensity. At a constant load current greater than zero, however, the relation between output voltage and illumination intensity becomes more complex.[1]

From these relations, it can be deducted that the effect of the illumination intensity on the current-voltage characteristic can be described closely by a displacement along the I-axis (Fig. 1). Test data show that such an approach is permissible for radiation intensities up to 120 mw cm^{-2} equivalent solar radiation.

When determining the output from a number of cells at different illumination levels, connected together in series or parallel, the use of current-voltage characteristics displaced as described above is of great help.

The irradiation density on cells on a spherical converter varies as the cosine of the angle of incidence of the radiation. The power output from uncoated and uncovered cells follows closely the irradiation density. For glass-covered cells, however, the reflectivity increases rapidly for angles of incidence larger than 65° and therefore, beyond this angle, the output power decreases faster than the cosine law would indicate.

Fig.1

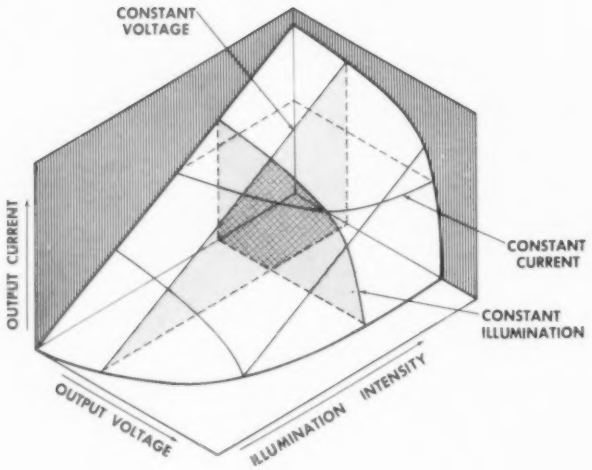

Fig.2

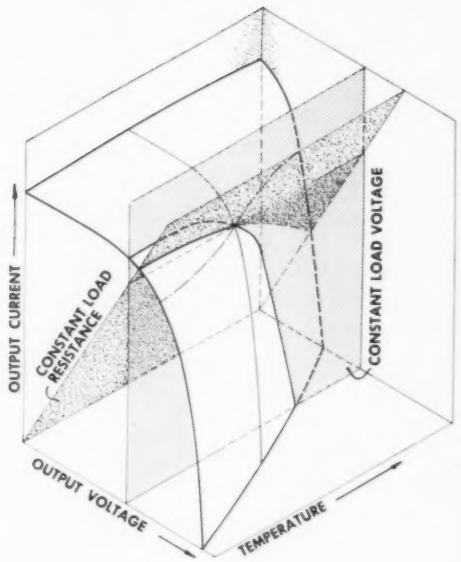

VOL. 4 1960

Fig.3

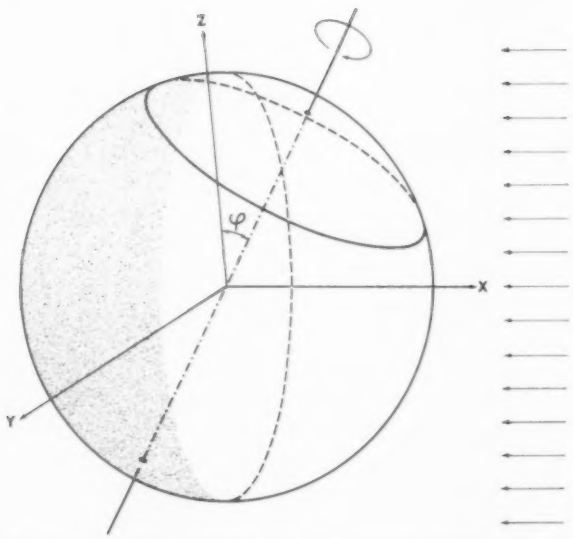

Fig.4

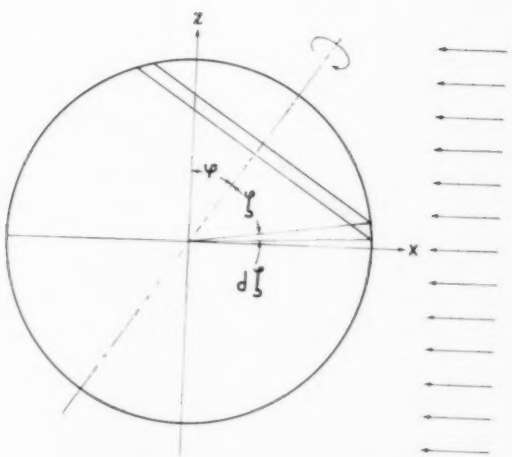

FIG. 1—Surface illustrating relation between output current, output voltage, and illumination intensity, at constant cell temperature.

FIG. 2—Surface illustrating relation between output current, output voltage, and temperature, at constant illumination.

FIG. 3—Sphere and rectangular coordinate system in space.

FIG. 4—Illustration of nomenclature for angles and surfaces.

TEMPERATURE INFLUENCE ON ELECTRICAL CHARACTERISTICS

As would be expected from a semiconductor device, the electrical characteristics of silicon solar cells are temperature dependent. In Fig. 2 the variation of the current-voltage characteristic with temperature is illustrated by the curved surface. The effect on output when solar cells are operated into a constant voltage load is indicated by the intersection of the vertical plane with the current-voltage surface. The rapid drop in output

current at higher temperatures should be especially noted.

Likewise, the intersection of the current-voltage surface with the plane representing constant resistance load, shows the temperature effect on output under such operating conditions. In neither case, does the variation follow the optimum power output (indicated by the dot-dashed line on the surface).

The temperature variation of short-circuit current, open-circuit voltage, and optimum power output have been described earlier in the literature.[1, 2, 3] For the optimum power output, the temperature coefficient is reported to be approximately $-0.6\%/°C$ in the temperature range -10 C to $+170$ C.

Recent measurements, however, indicate that the spectral response of silicon cells is temperature dependent; a higher temperature increases the long wave length response, shifting the response curve somewhat in the same direction. The temperature effects reported so far, were mostly determined with a tungsten filament source, either filtered through water or unfiltered. Since the tungsten lamp output peaks in the long wave region and sunlight has a totally different spectral distribution, especially in space, where it peaks at rather low wave lengths, it is apparent that the temperature coefficient for solar radiation in space will be greater than previous data indicate.

TEMPERATURE OF AN ENERGY CONVERTER ELEMENT IN AN EARTH SATELLITE

General Equation

To a first approximation, the temperature of an insulated element of a solar energy converter, such as a silicon solar cell, on an earth satellite can be expressed by:

$$T = \left[\frac{1-f}{\sigma}\left\{\left(\frac{A_\alpha}{A_\epsilon}\right)_S \frac{\bar{\alpha}_S}{\bar{\epsilon}_T} C_1 + \left(\frac{A_\alpha}{A_\epsilon}\right)_E \left(\frac{\bar{\alpha}_S}{\bar{\epsilon}_T} C_2 + \frac{\bar{\alpha}_E}{\bar{\epsilon}_T} C_3\right)\right\}\right]^{1/4} \quad [1]$$

where

T = Equilibrium temperature of element (K)
f = Fraction of incident energy converted and dissipated elsewhere
σ = Stefan-Boltzmann's constant ($5.67 \times 10^{-8} \text{wm}^{-2}K^{-4}$)
A_α = Projected absorbing area (m^2)
A_ϵ = Emitting area (m^2)
$\bar{\alpha}_S$ = Average absorptance for solar radiation
$\bar{\alpha}_E$ = Average absorptance for earth radiation
$\bar{\epsilon}_T$ = Average emittance of element at temperature T
C_1 = Direct solar irradiation (wm^{-2})*
C_2 = Earth reflected solar radiation (wm^{-2})*
C_3 = Earth long wave radiation (wm^{-2})*
and subscripts S and E refer to sun and to earth, respectively.

Equation [1] assumes that the heat transfer is accomplished only by radiation, without conduction of heat between the element and adjacent regions. Furthermore, it is assumed that no net radiation exchange occurs between various regions of the body of which the element under consideration is part, and also, that $\bar{\alpha}$ is independent of the angle of incidence. Finally, the effect of celestial bodies other than the sun and earth is neglected.†

Variation of Temperature with $\bar{\alpha}/\bar{\epsilon}$

It can be seen from Eq. [1], that, all other things being equal, the surface temperature is determined by the ratio of average absorptance to average emittance.

A decrease in temperature can therefore be achieved by decreasing the average absorptance or increasing the average emittance. As far as the output from silicon solar cells is concerned, the optimum ratio of $\bar{\alpha}_S/\bar{\epsilon}_T$ is 0.6. Presently, ratios of 1.0 or slightly less have been achieved.[6]

Variations of Temperature with A_α/A_ϵ

The ratio of projected absorbing area to emitting area can vary from unity to zero. According to Eq. [1], therefore, the temperature of an element can vary from a certain maximum to absolute zero.

The ratio A_α/A_ϵ for a surface element on a spinning sphere will vary with the element's position relative to the incident radiation. Assuming, however, that the spin rate is high compared with the thermal time constant, so that the temperature of ring elements taken perpendicular to the spin axis is virtually constant, it is sufficient to find the ratio A_α/A_ϵ for each infinitesimal ring element. Such assumption is realistic in most cases. For instance, a spin rate of 1.5 rpm on a sphere of 0.5 m radius with a silicon shell of 1 mm thickness and a mean temperature of about 300 K, would give a maximum temperature fluctuation of only about 6 C within any ring element.[7]

The ratio A_α/A_ϵ for any ring element normal to the spin axis can be determined for parallel radiation by the equations given in the methodological note (Pg. 39.) Figs. 3 and 4 show the geometry involved. The incident radiation, as symbolized by the arrows at the right, is normal to the Y-Z plane, and the spin axis lies in the X-Z plane, making an angle φ with the Z-axis. Any rotating sphere can be represented in this manner by

* Values for energy intercepted by a satellite on a 1000 mile orbit are given by Brettler[4] as: $C_1 = 1400\ \text{wm}^{-2}$; $C_2 = 160\ \text{wm}^{-2}$; $C_3 = 140\ \text{wm}^{-2}$.

† Camack and Edwards[5] give more detailed equations for the calculation of instantaneous temperature and discuss error sources in such calculations. A valuable list of references is also given therein.

turning the coordinate system around the X-axis until the sphere's axis of rotation lies in the X-Z plane.

The infinitesimal ring element is determined by the angle ζ from the spin axis, and has a width $d\zeta$. As shown on Pg. 39 the ratio $(A_a/A_e)_r$ can be expressed in terms of only these two angles, φ and ζ.

In Fig. 5, the variation of $(A_a/A_e)_r$ over the surface of a sphere is shown for several values of the angle φ from 0 to 90°. The greatest variation in $(A_a/A_e)_r$, and consequently in temperature, occurs when the spin axis is parallel to the incoming radiation, *i.e.*, for $\varphi = 90°$.

SERIES AND PARALLEL CONNECTION OF SOLAR CELLS

Matching Losses

When solar cells are connected in series or in parallel, the optimum output power of the cells will be less than the sum of the optimum output power from each individual cell unless the cells are properly matched. When considering this reduction of optimum power output it is convenient to use the concept of matching efficiency η_m. Matching efficiency is defined as:

$$\eta_m = P_{ab}/(P_a + P_b) \qquad [2]$$

where

P_a = Optimum power output from cell a
P_b = Optimum power output from cell b
P_{ab} = Optimum power output from cells a and b connected in parallel or in series.

The matching efficiency thus indicates how much of the possible power output is realized when cells are connected together.

Parallel Connection of Cells at Different Temperatures

When two solar cells or two series strings of cells at different temperatures but under equal illumination are connected in parallel, the matching efficiency is always below unity and drops with increased temperature difference. If the temperature difference between the cells or cell groups is great enough, the optimum power output from both cells or cell groups connected together may be less than the optimum power output from the one at the lower temperature.

Fig. 6 illustrates such a case. Cell A has a temperature of +130 C and an optimum power output of 20, as indicated by the shaded rectangular area. For Cell B, the corresponding numbers are +3 C and 72. Connected in parallel, the optimum power output is 50, obviously less than for Cell B alone. The matching efficiency in this case is 0.54.

The above example clearly illustrates that parallel connection does not always increase the output. If solar cells at different temperatures must be connected in parallel, it may be necessary to connect two or more cells at the higher temperature in series, before connecting them in parallel with cells at a lower temperature.

If the cell temperature varies, as on a rotating spherical collector, a rectifier element can be added to each series string of cells connected in parallel in order to avoid actual reduction in output power. The current-voltage characteristic (Fig. 6) for cells A and B connected in parallel then has the resultant shape shown in Fig. 7. Because of the voltage drop, and consequent power loss, over the rectifier element, such a solution is only adequate when series strings of five or more cells are connected in parallel.

Series Connection of Cells at Different Temperatures

For a series connection of cells at different temperatures but with equal illumination, area, and efficiency, the matching losses are negligible. In Fig. 6, Cells A and B connected in series have a matching efficiency of 0.98, compared to 0.54 when connected in parallel.

Series Connection of Cells at Different Illuminations

When two cells of same size, efficiency, *etc.*, are connected in series but illuminated with different intensities, the matching efficiency is less than unity and approaches zero when one cell is in the dark (Fig. 8).

It is therefore important to connect in series only cells which always receive approximately the same amount of radiation. On a cylindrical collector only cells lying on the same axial line, and on a sphere only cells within a small cluster, should be in series.

Parallel Connection of Cell at Different Illuminations

Under different illuminations, the matching losses for parallel connection of cells is much less than for series connection, and in practical applications they are reduced still further because the cells receiving less illumination are often operating at lower temperature and thus have a higher open circuit voltage (Fig. 8).

Series-Parallel Connection of Cells on a Spherical Converter

On a rotating sphere, except when the axis of rotation is parallel to the incoming radiation, cells having the same temperature do not receive the same amount of

FIG. 5—Numerical solution of Eq. [4] for several values of φ.
FIG. 6—Effects of parallel and series connection of solar cells at different temperatures.
FIG. 7—Effects of parallel connection when using blocking diodes.
FIG. 8—Effects of parallel and series connection of solar cells at different illumination levels.
FIG. 9—Illustration of nomenclature used in the sample calculation.
FIG. 10—Current-voltage characteristics for each of five bands and overall characteristics for parallel connection.

VOL. 4 1960

Fig.5

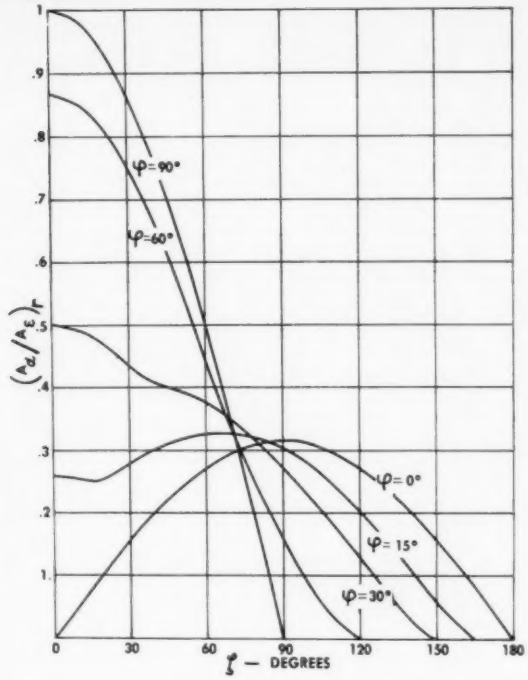

Fig.6

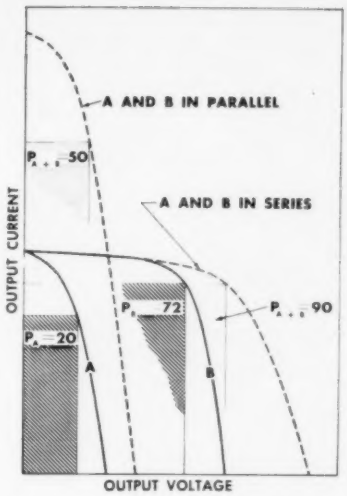

Fig.7

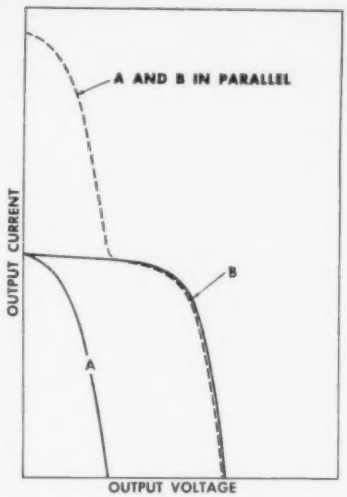

Fig.8

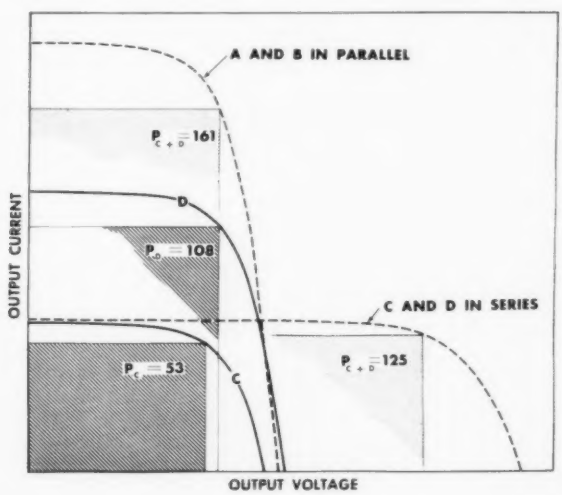

Fig.9

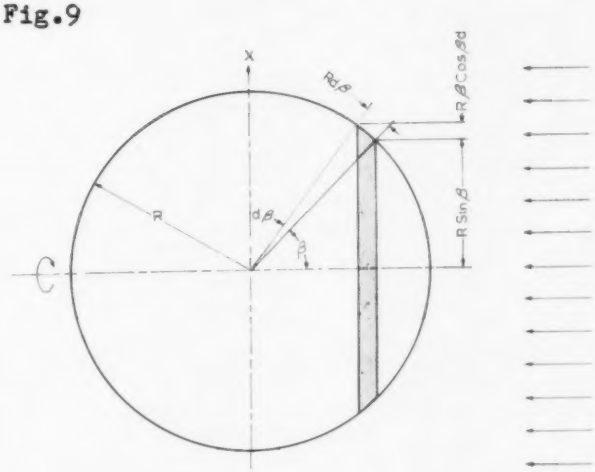

Fig.10

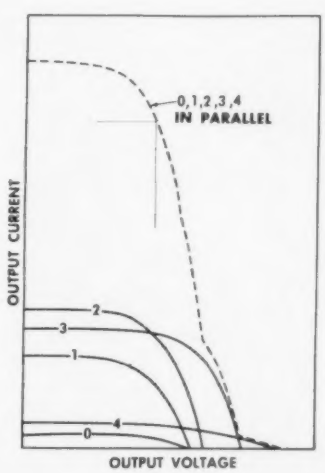

FIGS. 5-10

irradiation at each instant. This phenomenon results because the temperature is uniform for ring elements normal to the spin axis whereas the irradiation is constant for ring elements normal to the direction of the incoming rays.

The problem, then, is that of series-parallel connecting cells at both different temperatures and different illuminations. And a lower illumination level does not always correspond to a lower temperature.

The effective illumination profile is always the same over the sphere relative to the incoming rays, and it follows closely the cosine of the angle of incidence at each point. Solar cells, however, are frequently covered with glass or quartz covers, and here the reflectivity increases rapidly for angles of incidence greater than 65°. The effective illumination, therefore, decreases faster than the cosine law for angles above 65 degrees.

The temperature profile varies with the angle φ (Fig. 5). The worst case as far as power output is concerned arises when φ is 90°, *i.e.*, when the spin axis is parallel to the incoming radiation.

For reasons stated above, every cell in a series string must receive the same amount of illumination to yield optimum performance. Each series string should consequently extend only over a limited surface area. This requirement limits the number of cells which can be connected in series. In addition, each series string must be connected to a rectifier cell, to prevent power losses through strings under low illumination intensity.

CALCULATION OF POWER OUTPUT

The minimum output from a spherical converter completely covered with cells occurs when the angle φ is 90°. To a first approximation, the power output for this case can be determined in the manner described below.

Subdivide the sphere into a number of bands of equal width, $Rd\beta$, as shown in Fig. 9. The width should be so chosen that the smallest band contains just *one* string of N cells connected in series.

The projected area, F_1, of this band is determined by:

$$F = \pi R^2[\sin^2(\beta + d\beta) - \sin^2\beta] \qquad [3]$$

while the temperature, T_1, is calculated from Eq. [1]. These two parameters, projected area and temperature, determine the current-voltage characteristic for this band.

The second band, having a projected area of F_2, will have a short-circuit current F_2/F_1 times that of the single series string. Note, however, that the number of parallel-connected strings (each string consisting of N cells) of the second band is proportional to the ratio of the actual (not projected) area of this band relative to the first.

Continuing in this fashion, the output characteristics for all bands over the illuminated hemisphere are obtained. Since all series groups are connected in parallel, the total output characteristic for the sphere is obtained by adding the characteristics of each band. This is done graphically, as described previously under the heading Parallel Connection.

Determination of the output for any other value of the angle φ is much more complicated. In this case, the illumination and temperature must be calculated separately for every series string.

Example of Power Output Calculation

This sample calculation illustrates the step-by-step calculations for the case of $\varphi = 90°$. Assume that $d\beta$ for *one* series string of cells is 20°. By Eq. [3], the projected area of each of the five bands is:

$$F_1 = 0.0299\pi R^2$$
$$F_2 = 0.2201\pi R^2$$
$$F_3 = 0.3367\pi R^2$$
$$F_4 = 0.2968\pi R^2$$
$$F_5 = 0.1165\pi R^2$$

The normalized projected area relative to F_1 for these bands is:

$$F_1/F_1 = 1$$
$$F_2/F_1 = 7.35$$
$$F_3/F_1 = 11.28$$
$$F_4/F_1 = 9.92$$
$$F_5/F_1 = 3.90$$

These values will determine the relative short-circuit current for the various bands. Because of the increased reflectance, the output current for band 5 is assumed to be only 50 per cent of the value indicated above; that is, $(F_5/F_1)_{corr} = 1.95$.

The temperature is assumed to vary only as the ratio $(A_\alpha/A_\epsilon)_r^{1/4}$. For a ratio of $\bar{\alpha}/\bar{\epsilon} = 1$, and neglecting radiation other than that of the sun, the temperature of the bands, according to Eq. [1] and with $C_1 = 1400$ wm^{-2} and $f = 0.10$, will be:

$$T_1 = 113\ \text{C}$$
$$T_2 = 107\ \text{C}$$
$$T_3 = 88\ \text{C}$$
$$T_4 = 51\ \text{C}$$
$$T_5 = 23\ \text{C}$$

Temperature will affect the output characteristics as was noted earlier.

The effect of incident radiation is shown in Fig. 1. We are interested in the open-circuit voltage, and the sequence used to find this voltage is to determine it at normal incidence at the actual temperature, and then to adjust it with reference to the angle of incidence. This method is illustrated as follows.

From a plot* of actual I-V characteristics for different temperatures and at the illumination intensity

* Plots of typical I-V characteristics for solar cells are usually available from the manufacturer.

VOL. 4 1960

in question, the voltages at normal incidence are obtained for the strings in each band. In the present case, they are:

$$(V_1)_n = 0.33N$$
$$(V_2)_n = 0.35N$$
$$(V_3)_n = 0.39N$$
$$(V_4)_n = 0.48N$$
$$(V_5)_n = 0.67N$$

where N is the number of cells in series per string, and n refers to normal incidence conditions.

Because of varying angle of incidence, the voltage from each band will be less than for normal incidence. This reduction is determined graphically using the I-V plot. In the present case we have:

$V_1 = 0.33N$
$V_2 = 0.34N$
$V_3 = 0.37N$
$V_4 = 0.44N$
$V_5 = 0.51N$ (including the effect due to increased reflection)

Since each string has one blocking diode in series, the forward voltage drop of each diode must be subtracted from the above voltages.

Finally, knowing the short-circuit current and the open-circuit voltage for each band, the characteristics of each band can be drawn with the aid of the previously mentioned I-V plot. These band characteristics are now added in parallel to yield an over-all characteristic for the sphere, from which the optimum power output and corresponding load resistance is determined. This procedure is illustrated in Fig. 10.

Acknowledgment

The helpful suggestions of C. A. Escoffery and M. F. Gift are gratefully acknowledged.

METHOLOGICAL NOTE ON RATIO OF PROJECTED ABSORBING AREA TO EMITTING AREA OF RING ELEMENTS ON A ROTATING SPHERE.

As seen from Fig. 4, for the case of $(\pi - \varphi) \geqq \zeta \geqq \varphi$ the projected absorbing area of one ring element is equal to

$$A_{ar} = 2R^2 \sin \zeta d\zeta [\cos \zeta \sin \varphi(\pi - \Theta) + \sin \zeta \cos \varphi \sin \Theta]$$

where $\Theta = \arccos (\tan \varphi / \tan \zeta)$. For $\zeta \leqq \varphi$, it is

$$A_{ar} = 2\pi R^2 \sin \zeta \cos \zeta \sin \varphi \, d\zeta$$

and for $(\pi - \varphi) \leqq \zeta \leqq \pi$, it is

$$A_{ar} = 0$$

The emitting area of one ring element is:

$$A_{er} = 2\pi R^2 \sin \zeta \, d\zeta$$

Therefore, the ratio of the projected absorbing area to the emitting area of each ring element is given, for $(\pi - \varphi) \geqq \zeta \geqq \varphi$, by

$$(A_a/A_e)_r = [\cos \zeta \sin \varphi(\pi - \Theta) + \sin \zeta \cos \varphi \sin \Theta]/\pi \quad [4]$$

For the case of $\zeta \leqq \varphi$, it is given by

$$(A_a/A_e)_r = \sin \varphi \cos \zeta$$

and finally, for $(\pi - \varphi) \leqq \zeta \leqq \pi$, it is given by

$$(A_a/A_e)_r = 0$$

REFERENCES

1. Prince, M. B., and Wolf, M., "New Development in Silicon Photovoltaic Devices", *J. Brit. IRE*. **18,** 583 (1958).
2. Nash, H. and Luft, W., "Improved Silicon Photovoltaic Cells for Space Vehicles", *Electronics Industries*, **18,** 91 (1959).
3. Luft, W. and Nash, N., "Temperature Control of Silicon Solar Cells in Space Environment", *Semiconductor Products*, **3,** 39 (1960).
4. Brettler, *et al.*, "Geodetic Satellite Flashing Light System Study," Part I, Design and Feasibility Studies; Report No. B-1966A, Contract No. Nonr-2954(00) (X); Office of Naval Research, Wash. D. C., September 30, 1959.
5. Camack, W. G. and Edwards, D. K., "Effect of Surface Thermal-Radiation Characteristics on the Temperature-Control Problem in Satellites", p. 3, in *Surface Effects on Spacecraft Materials*, F. J. Clauss, Editor; John Wiley & Sons, New York, 1960.
6. Escoffery, C. A. and Luft, W., "Optical Characteristics of Silicon Solar Cells and of Coatings for Temperature Control," *Solar Energy*, **4,** (1960).
7. Charnes, A. and Raynor, S., "Solar Heating of a Rotating Cylindrical Space Vehicle," *J. Am. Rocket Soc.* **30,** 479 (1960).

Solar Abstracts

Prepared by Milton D. Lowenstein, Director, Technical Research Service Center

Abstracts, it may be observed, are useful to the extent that they are readily available at those critical moments in research and development activities when the advancement of a project depends upon objective and well recognized authority.

The Solar Energy Technical Research Service Center is establishing a source of information and a routine for supplying data as soon as they are received and processed. All the material in the library, correspondence on technical matters and research reports are being classified and arranged for quick retrieving of useful information.

As a record of each member's fields of interest is in our file, appropriate data can be expedited to where they may be needed. "Uniterm" type and punch card systems and ultimately computers will aid in the retrieving process.

Until the system is fully organized, members will receive, periodically, bibliographies of current literature in the Research Service Center library of AFASE. The most important of these papers will be abstracted for the Journal.

Your suggestions for further improvements will be welcomed by the director of the Technical Research Service Center.

---

* * *

Low Temperature

Burdick, Glydewell; Smith, Howard S.; Olson, Floyd. "Electric Heating Forum, No. 1". *Electrical Construction and Maintenance*, July 1960.

A breakdown of metered annual heating energy for heavily insulated houses into component heat losses and heat gains is given in the article "Design Heat Losses and Annual Energy Requirements" by Glydewell Burdick. The development of a curve showing the variation in the NEMA formula constant with the design heat loss of a residence is presented in "Design Heat Loss and the NEMA Constant" by Howard S. Smith and Floyd Olson.

* * *

Heywood, J. B. "The design of a solar water still", *Cambridge University Engineering Society*. 10 p. illus.

A simple roof type still which uses "the glasshouse effect" to trap radiation will be considered in this paper. The essential features of a still of this type are an evaporator and a condenser. The first usually consists of a shallow pan, or suspended pad, filled or saturated with saline water which serves as an absorber of solar radiation. The second is usually an inclined or curved transparent surface which hermetically seals the evaporator. This transmits the solar radiation, and allows wind cooling to dissipate the heat evolved by the condensing vapour.

* * *

Stroebel, Joseph J.; Sieveka, Ernest H.; Sandell, Dewey J., Jr.; Bradt, David M.; Lof, George O. G. "Review of desalinization processes", panel discussion. *Journal American Water Works Association*, vol. 52, No. 5, May 1960. 32 p. illus.

A panel discussion presented on October 21, 1959, at the joint meeting of the Alabama-Mississippi and Southwest sections, New Orleans, La. The discussion covers the articles "Recent Developments" by Joseph J. Strobel, "Membrane Processes" by Ernest H. Sieveka, "Freezing Processes" by Dewey J. Sandell, Jr., "Distillation Processes" by David M. Bradt, and "Solar Distillation" by George O. G. Lof.

* * *

Medium Temperature

Belikova, V. K. "The bactericidal significance of solar radiation penetrating a room". Distributed by the Office of Technical Services, U. S. Department of Commerce. December 1958. JPRS: L-547-N. 9 p.

From the point of view of hygiene, great interest attaches to the problem of the bactericidal effectiveness of solar radiation penetrating into a room and to its role in the general bacterial decontamination of the air. There are indications in the literature of the fact that the action of ultraviolet rays may reduce the aggressive properties of bacteria and render their toxins innocuous without influencing their antigenic and immunologic properties. The experiments were run on two virulent cultures: the pyogenic Staph. albus, and B. Breslau. The conclusion is that long-wave ultraviolet radiation from the sun, passing through window glass, has a bactericidal action. Upon irradiation of a room with such rays for a period of three hours, an effective bactericidal action is achieved. Studies conducted for this purpose provide a basis for the determination of hygienic requirements for minimal durations of solar irradiation of rooms both in houses and in public buildings.

* * *

Morse, R. N. and Czarnecki, J. T. "Flat plate solar absorbers: the effect on incident radiation of inclination and orientation" sponsored by the Commonwealth of Australia, August 1958. Report E. D. 6. 26 p. illus.

The influence of inclination and orientation of the receiving surface on the amount of incident solar radiation is examined. An expression is derived which enables the angle of inclination for maximum insolation over any period of time to be evaluated. The inclination for equal insolation at summer and winter solstices is also determined. Information for designers of absorber installations is given in the form of curves showing insolation throughout the year for a series of surfaces at different angles of inclination and varying in orientation. It is

VOL.
4
1960

shown that neither inclination nor orientation is as critical as has been thought.

* * *

High Temperature

Athay, R. G. "H^{β}, H^{γ}, and K Profiles in Chromospheric Spicules", Extrait *des Annales D'Astrophysique,*" Tome 23, No. 2, Mars-Avril, 1960, p. 1–12. illus.

The study of line profiles for chromospheric spicules is extended to the H^{β}, H^{γ} and K-lines. Earlier observations of the D_3 line in conjunction with the H^{β} and H^{γ} lines indicates a kinetic temperature of about 50,000°.

The K-line is found to have anomalous broadening from a non-thermal velocity field not shared by hydrogen and He I. This velocity field of the Ca II ions is tentatively identified with the interaction of Ca II ions with magnetic fields.

* * *

Athay, R. Grant. "The Equilibria and Ultraviolet Spectra of H, He I, and He II in the Solar Atmosphere, *The Astrophysical Journal,* Vol. 131, No. 3, May 1960, p. 705–16. illus.

The ionization equilibrium equations and source functions for the ions H, He I, and He II are considered under conditions appropriate to the solar chromosphere. The equations are formulated in terms of both occupation numbers and b_k parameters, in order to clarify their relationship to earlier work for H and He I. In the case of the ionization equations for H, somewhat more approximate forms are adopted from those appearing in earlier works, in order to illustrate more clearly the dominant transitions in the equilibrium. The three ions considered here exhibit fundamental differences as well as many similarities in both the ionization equations and the source functions.

A consideration of the ultraviolet spectra indicates that the central intensities in the Lyman-β lines are influenced mainly by the "local" value of Te, near the region t-1, whereas the central intensities of the Lyman-a lines are influenced by the distribution of T, throughout a large range in r and cannot be described solely in terms of the "local" value of Te, near r-1. For this reason, observations of the Lyman-β profiles and fluxes by means of rockets and satellites become a much more valuable supplement to Lyman-α observations than had previously been supposed.

* * *

Photoelectric

Rudenberg, H. G.; Dale, B. "Photovoltaic Conversion 17–18–19", *Proceedings 14th Annual Power Sources Conference,* May 1960, 4. illus.

A research and development program has been in progress at Transitron for a year on improved photovoltaic solar energy converters. At the beginning of this work, silicon solar cells of 8–10% conversion efficiency were readily produced with occasional accidents providing spectacular 14% efficiency. The major limitations and improvement factors were then known, but much detailed work in applying these properly remained to be done. The initial analysis of the problem followed well known outlines; however, the work at Transitron departed from the conventional in several areas to establish new approaches toward the goal of high efficiency, high yield and low cost on a laboratory basis. Table 1 summarizes the improvement factors obtained to date, and the approach toward the theoretical ideal conditions.

* * *

Witt, Von H. T.; Moran, R.; Muller, B.; Zieger, Rumberg Und G. "Kinetische Untersuchungen uber die Primarvorgange der Photosynthese", *Zeitschrift fur Elektrochemie-Berichte der Bunsengesellaschaft fur physikalische Chemie,* Band 64, Heft 1, 1960 (Seite) p. 181–87. illus.

By use of a suitable flash method four types of absorption changes were found during photosynthesis in plant cells. Type 0 and Type 1 describe two reactions on chlorophyll. Type 2 is connected with the decomposition of water. Type 3 describes the course of a redox reaction at the end of the primary.

* * *

Wolf, M. "Limitations and possibilities for improvements of photovoltaic solar energy converters", *The Proceedings of the IRE,* July 1960, p. 20. illus.

Seven factors limiting the performance of photovoltaic solar energy converters are listed and explained. They can be classified into basic and technology determined limitations. Possibilities for improvement on technology determined limitations are investigated for the silicon solar cell. Such possibilities are: heavier *p*-layer doping; change of geometry, possibly by application of grid structures; improvement of the material constants; and utilization of drift fields for improved collection. Discussed are materials other than silicon in regard to their potential for better performance than that obtainable from the silicon solar cell; and finally, new methods of approach, such as the multilayer and the multiple transition solar cell. Both of these methods yield theoretically large improvements, but realization depends on further advances in compound semiconductor technology and in knowledge about localized centers in the forbidden gap. Limit conversion efficiencies of 38.2 per cent for a 3-transition cell, compared to 23.6 per cent for a single p-n junction, single transition cell, are obtained. Also discussed are the possible merits of the application of the graded energy gap to photovoltaic energy converters, and potential improvement in collection efficiency is found for certain cases.

* * *

Wysocki, J. Loferski; Rappaport, P. "Research on Photovoltaic Converters", *Proceedings 14th Annual Power Sources Conference,* 17–18–19 May 1960, 5 p. illus.

This paper is a summary of the research performed on solar energy converters at the RCA Laboratories during the past year. The major effort has been on Ga for solar cells, although some work has been done on other materials such as GAP. Other solar energy schemes have been considered; in particular, the PEM (photo-electromagnetic) energy converter. Some remarks are made on the question of standard cells and calibration using artificial sunlight sources.

* * *

Economic, Social and Cultural Parameters

Angstron, A. K. and Drummond, A. J. "Transmission of "cutoff" glass filters employed in solar radiation research". *Journal of the Optical Society of America,* Vol. 49, No. 11, November 1959, 3 p. illus.

The temperature dependence of the wavelength position of the lower sharp cutoff of Schott glass filters and, in particular, the OGI type is discussed. Generalized relationships are developed to represent the measured filter transmissions. The principal results for the OGI, RG^2, RG^3 filters are presented in tabular form.

* * *

Laszlo, Tibor S. "On radiant energy in high-temperature research". ASME publication. paper number 60-WA-170. 7 p. illus.

A completely fresh approach has to be taken for each type of experimentation when using high-intensity radiant energy.

The size, shape and mounting of the specimen may require unconventional arrangements. New methods of observation and measurements must be developed together with instruments of special design. Because of the novelty of image furnaces, very little of this has been done up until the present time. However, with progress in this field a unique and very versatile tool will soon be available for high-temperature research. During the present investigations a new shape for artificial black bodies was conceived, consisting of a truncated right cone with the smaller end as the orifice.

* * *

Novak, W. J. "Electric heat can cost less than conventional estimates indicate." *Electrical Construction and Maintenance*, April 1960. 5 p. illus.

Solar electric heat and insulation, Salt Lake City, Utah, has reduced heating operating costs to all-time lows using rigid construction specifications, progressive insulating techniques, and a conscientious follow-up. Submetering provides accurate data on validity of estimating methods used.

* * *

Materials

Knezevich, S. J. "Glass, the controversial school building material". *School Board Journal*, July 1960. 4 p. illus.

An analysis of the three major problems of our "glassical" schools: daylighting control, solar heat gain, and interior heat loss.

* * *

Accessories

Schipper, Leon. "Weight optimization of a solar or nuclear mechanical conversion system". Wright Air Development Center, June 1959. 50 p. illus.

Energy conversion systems for spacecraft must provide required power with minimum weight. Parameters are investigated for obtaining optimum weight. Efficiency of a component, group of components, or the entire system is important only insofar as it minimizes over-all system size and weight. Basic parameters are established for a solar-powered system and specific values assigned. The effect of varying the parameters contributing to efficiency versus system weight are noted. The variables contributing most to system size and weight are collector and radiator. For a nuclear-powered system, the radiator is the only variable providing a possibility of significant weight reduction. By properly matching the parameters affecting the power-producing unit with parameters affecting the heat-rejecting unit, optimum system weight can be achieved.

* * *

Simmonds, James G. "The dynamics of large rotating membrane-like structures". IAS paper no. 60–87. 16 p. illus.

In this paper the purpose was first to derive, from the exact equations, a rational set of approximate equations governing the arbitrary motion of rotationally symmetric membranes. Second, after pointing out a few of the inherent difficulties involved in solving the general equation, we analyzed the simplest, nontrivial case of these equations available—the flat disk. And third we showed by means of our dynamic analysis that at certain rotational speeds the disk became elastically unstable. By inference we concluded that this type of instability would exist in more general membrane configurations than the flat disk and, for relatively small hubs, would limit their maximum rotational speeds.

Geophysical and Astronomical

Babcock, Harold D. "The Sun's Polar Magnetic Field", *The Astrophysical Journal*, Vol. 130, No. 2, September 1959, p. 364–65. illus.

The polarity of the high-latitude dipolar magnetic field of the sun was opposite to that of the earth's field from 1953 to 1957. About the middle of 1957, the polarity of the magnetic field near the south heliographic pole was reversed; reversal of the field near the north pole was not observed until November, 1958. At present, the sun's polar field is parallel to that of the earth.

This paper presents new data on the weak persistent magnetic fields characteristic of high heliographic latitudes.

* * *

Matsushita, S. "Studies on Sudden Commencements of Geomagnetic Storms Using IGY Data from United States Stations", Journal of Geophysical Research, Vol. 65, No. 5, May 1960, 1423–35 pp. illus.

This report contains studies of geomagnetic storm variations recorded at a network of seven IGY stations in the United States together with records for other observatories operated by the United States. The distance between adjacent stations of the network ranges from 360 to 510 km. Geomagnetic variations at the stations were usually quite similar, as would be expected. During magnetic storms, however, remarkable differences occurred even between adjacent stations.

About half of the sudden commencements of the horizontal component showed different shapes at adjacent stations for the same magnetic storm. From the data obtained from these results, and from observations at more distant stations, the behavior of sudden commencements is examined. The data also show that the variations of the vertical component of the sudden commencement differ in ways suggesting notable irregularities of the earth's conductivity in the central part of the United States. In addition, occasional examples of bay-shaped variations during magnetic storms, which are quite nonuniform over the closely spaced net, are illustrated and analyzed.

* * *

Athay, R. Grant; Johnson, Hollis R. "The Excitation of He 1 in the Solar Spectrum", *The Astrophysical Journal*, Vol. 131, No. 2, March 1960, p. 413–28. illus.

The excitation and ionization of He 1 in the solar atmosphere is computed for a range of values of n_e and T_e and the radiation field in the resonance lines. Good agreement is found between the observed and computed b_{1s} parameters for T_e 40000°–50000° and n_e 10^{11}. The criterion for the 10830 and X 5876 lines to show as emission lines against the solar disk is found to be n_e 10^{12} almost independently of T_e.

* * *

Bonnaud, Paymal; Clerc, P. Le., "Radiation Dosimeter Glasses", August 1960, p. 430–36. illus.

Ionizing radiations produce visible colors in glasses containing certain multiple valence ions. The coloration, which is dependent on the radiation dose, is generally unstable. Combinations of certain ions can produce glasses with sufficient color stability to be used as dosimeters. Combinations of Mn-Fe, Mn-V, and Mn-V-Fe were studied. The response of glasses containing Mn-V-Fe, was independent of the intensity of radiation and they may be used in the range between 10^5 to 2×10^7 roentgens.

* * *

Ganivoort, Noble C. Billings, Donald E. "Prominence Characteristics in Regions of Bright Coronal Emis-

VOL. 4 1960

sion", *The Astrophysical Journal*, Vol. 132, No. 1, July 1960, p. 213–17. illus.

Prominences showing a high degree of fragmentation and large internal motions are found to be most prevalent in regions of high coronal density. The relative prevalence of other types of prominences in such coronal regions is also considered. We conclude that prominences which carry matter in greatest quantities from the corona to the solar surface are those which are located within regions of high coronal density.

* * *

Hirt, R. C.; Schmitt, R. G.; Searle, N. D.; and Sullivan, A. P. "Ultraviolet Sprectral Energy Distributions of Natural Sunlight and Accelerated Test Light Sources," *Journal of the Optical Society of America*, Vol. 50, No. 7, 706–713, July, 1960.

A contributory factor to the failure of correlation between outdoor and indoor photodecomposition tests is the difference in the ultraviolet spectral energy distributions of natural sunlight and the various indoor test sources which do not duplicate sunlight and differ widely among themselves. The ultraviolet spectral energy distributions of natural sunlight and of a variety of indoor exposure test sources have been measured. By use of a ferrioxalate actinometer, the measurements have been put on an absolute basis permitting the intercomparison of the sources. The xenon arc was found to be the best approximation of sunlight in the ultraviolet. For shorter-wavelength ultraviolet (below 3500 A), the combination of fluorescent sunlamp and blacklight lamps also approximated sunlight.

* * *

Jensen, A. S.; Limansky, I. (Westinghouse Electric Corporation) "Photoelectric Conversion", *Proceedings 14th Annual Power Sources Conference*. May 1960, 4 pp. illus.

The photoelectric phenomenon appears to hold excellent promise as a method of utilizing solar energy. Since the main objection to present day photoelectric devices is their high internal impedance, a careful mathematical analysis was instituted which showed that close spacing of the anode and cathode, a low work function material for the anode, and the use of a screen to keep the anode in the dark combine to make a low-impedance generator with useful efficiency. Using presently available materials, the analysis shows that a photoemisive power generator can be made, capable of delivering approximately 3 per cent of the incident solar power to a matched load. This is an output of 1 kw from about 250 ft.^{2}.

* * *

Karoli, A. R.; Angstrom, A. K.; Drummond, A. J. "Dependence on atmospheric pressure of the response characteristics of thermopile radiant energy detectors". *Journal of the Optical Society of America*, Vol. 50, No. 8, p. 7. illus.

An account is given of an investigation into the pressure dependence of the sensitivity (i.e. responsivity) of 10 different types of thermopile detector over the pressure range 760 10^{-5} mm. The study is confined to those forms of thermopile commonly used for the measurement of unmodulated solar and infrared radiation. The radiation intensity-thermopile emf relationship at reduced ambient pressures is discussed, as is also the change introduced into the response-time constant. It is demonstrated that the results for the different instruments are in agreement, generally, with what is derived from the fundamental laws governing energy transfer within radiometric devices.

Katz, Arthur J. "Determination of thermal radiation incident upon the surfaces of an earth satellite in an elliptical orbit," IAS paper no. 60–58. 16 p. illus.

The thermal radiation incident upon arbitrarily chosen areas of an orbiting satellite can be determined when the motion and attitude of the satellite are known. The orbit is assumed to be elliptical and the incident radiation is determined for a non-rotating and "downward-looking" satellite. Radiation from the parent body about which the satellite revolves, the sun, and that solar radiation reflected by the parent body, are computed as a function of the location of the satellite in orbit. The radiation emitted by and reflected by the parent body is determined by integrating the incremental radiation over the entire spherical cap "seen" by the satellite. The intensity of solar radiation is assumed constant except that shadow areas are accounted for. A satellite coordinate system is established based on orbital parameters such that the satellite moves in a coordinate plane. The system rotates with the satellite so that the satellite radius vector remains co-linear with one of the axes. The method is applied to a hypothetical satellite in the orbit of 1959 alpha one. Comparisons are made between the radiation to a rotating and a non-rotating satellite. Generalized curves are shown, from which preliminary design information can be gotten for any satellite.

* * *

Malville, J. M. "Narrow Hydrogen Emission in the Aurora", *Planet, Space Sci.* Pergamon Press, 1960. Vol. 2, p. 130–32. illus. Printed in Great Britain.

In the southern auroral zone during the winter of 1957, H. was detected which had a width equal to or less than 8A. This observation is viewed as evidence for proton bombardment without the usual high velocity auroral particles. The alternate explanation of enhanced fluorescence of interplanetary hydrogen is discussed.

* * *

McCaulley, J. W.; Roach, P. E., Matsushita, S. "A study of Local Geomagnetic Influence on the (01) 5577 Nightglow Emission at Fritz Peak", *Journal of Geophysical Research* Vol. 65. No. 5, May 1960. p. 1499–1501. illus.

A comparison is made of (1) the horizontal magnetic intensity at Leadville, Colorado, and (2) the absolute zenith intensity of (01) 5577 at Fritz Peak, Colorado. The absolute zenith intensity of 5577 tends to increase as the magnetic H becomes more negative.

* * *

Roberts, Walter Orr; Zirin, Harold. "Recent Progress in Solar Physics", *Journal of Geophysical Research*, Vol. 65, No. 6, June 1960. p. 1645–59. illus.

A number of significant recent advances in solar physics are reviewed. New kinds of observations made during the present sunspot cycle, which began in 1954, have emphasized still further the apparent complexity of solar phenomena and the need of nonequilibrium theoretical treatments. Among the new developments discussed are solar cosmic rays and high-energy particles, flares and prominences, coronal condensations, solar magnetic fields, and solar radio noise emission. Theoretical analyses of the conditions of the solar atmosphere as a hot plasma, and as a gaseous ensemble exhibiting gross departures from thermodynamic equilibrium are discussed. New work on atomic collisional parameters is also reviewed. The article concludes with a synopsis of certain major unsolved problems of the solar atmosphere.

* * *

Zirin, Harold; Einar Tandberg-Hanssen. "Physical Conditions in Limb Flares and Active Prominences

IV. Comparison of Active and Quiescent Prominences", *The Astrophysical Journal*, Vol. 131, No. 3, May 1960, p. 717–24. illus.

Spectra of active and quiescent prominences appearing simultaneously at the limb of the sun are analyzed and discussed. The quiescent prominence shows a spectrum identical with that of the chromosphere at 1500 km, with strong lines of H, He I, and ionized metals and weak He II. The active prominence shows strong He II and very weak ionized metal lines. The lines in the active prominence are very much broader. The width of lines in wither prominence is shown to depend on their excitation potential. It is proposed, as a result of many observations, that, except for strong lines such as those of hydrogen and Ca II, the spectra of prominences fall into two sharply defined classes, depending on whether they are "hot" or "cool."

VOL.
4
1960

OL.
960